Event-Triggered Adaptive Control of Coupled Hyperbolic PDEs With Piecewise-Constant Inputs and Identification

Ji Wang, *Member, IEEE*, and Miroslav Krstic, *Fellow, IEEE*

***Abstract*—In this article, we present an event-triggered boundary control scheme with a, likewise, event-triggered batch least-squares parameter identification for a 2×2 hyperbolic PDE-ODE system, where two coefficients of the in-domain couplings between two transport PDEs, and the system parameter of a scalar ODE, are unknown. The triggering condition is designed based on evaluating both the actuation deviation caused by the difference between the plant states and their sampled values, and the growth of the plant norm. When either condition is met, the piecewise-constant control input and parameter estimates are updated simultaneously. For the closed-loop system, the following results are proved: first, the absence of a Zeno phenomenon; second, finite-time exact identification of the unknown parameters in most situations; third, exponential regulation of the plant states to zero. In the numerical simulation, the design is verified in an application of axial vibration control of a mining cable elevator, where the damping coefficients of the cable and the cage are unknown.**

***Index Terms*—Adaptive control, backstepping, event-triggered control, hyperbolic PDEs, least-squares identifier.**

I. Introduction

A. Motivation

A MINING cable elevator is a vital device used to transport the minerals and miners between thousands of metres underground and the ground surface [37]. Cable plays an indispensable role in the mining elevators due to its advantages of resisting relatively large axial loads and low bending and torsional stiffness, which are helpful to transporting heavy load in large depth. However, the compliance property or stretch and contract abilities of cables tend to cause mechanical vibrations, which may lead to premature fatigue fracture. Active vibration control is one economic way to suppress vibrations in the mining elevator because the mechanical structure of the elevator does not need to be changed.

The vibration dynamics of the mining cable is originally described by a second-order hyperbolic PDE [37], which can be converted into a class of coupled transport PDEs [8], [10], [11], [20], [36] in the Riemann coordinates [28]. Based on the coupled transport PDE system with fully known plant parameters, boundary control strategies were proposed for cable-actuated mechanisms to suppress the axial vibrations in [43], and the axial-lateral coupled vibrations in [38]. In practice, however, there always exist some plant parameters not known exactly, which create significant challenges for the control design and analysis, creating a need for adaptive technology. Three traditional adaptive schemes are the Lyapunov design, the passivity-based design, and the swapping design, which were initially developed for ODEs in [25], and extended to parabolic PDEs in [26], [32], and [33], and hyperbolic PDEs in [1], [5] and [7].

The adaptive control system for mining cable elevators includes the plant states, namely, the vibration states of the cable and cage, and the adaptive estimates for unknown parameters. Since both the undesired vibrations and the learning transient in the adaptive estimates include high-frequency signals, difficulties may arise in implementing the adaptive control laws in the practical mining cable elevators because the massive actuator, consisting of the hydraulic cylinder and head sheave (shown in [39, Fig. 1]), is incapable of supporting the frequently and fast changing control signal. Moreover, such a control input may in turn become a vibration source for the cable, and cause resonance. This motivates us to design a control law where both the plant states and the parameter estimates are piecewise-constant.

B. Event-Triggered Control of PDEs

In comparison with using periodic sampled-data control [9], [16], where unnecessary and energy-intensive movements of the massive actuator may appear, the event-triggered control is preferable for the mining cable elevator, where the massive actuator only moves at the necessary times determined by evaluating the operation of the elevator.

Most current designs of event-triggered control are for ODE systems, such as in [17], [19], [30], and [34]. For PDE systems, event-triggered control schemes were proposed for distributed (in-domain) control of PDEs in [29] and [44]. For the boundary control of PDEs, event-triggered boundary control of hyperbolic PDEs and parabolic PDEs, was originally proposed in [13] and [15], respectively. For a class of 2×2 coupled linear hyperbolic PDEs considered in this article, the event-triggered boundary control designs were presented in [12], [14], and [39].

Manuscript received 8 May 2021; revised 19 December 2021; accepted 20 February 2022. Date of publication 15 March 2022; date of current version 28 February 2023. This work was supported by National Science Foundation under Grant 1935329. Recommended by Associate Editor M. Guay. *(Corresponding author: Ji Wang.)*

Ji Wang is with the Department of Automation, Xiamen University, Xiamen 361005, China (e-mail: jiwang9024@gmail.com).

Miroslav Krstic is with the Department of Mechanical and Aerospace Engineering, University of California, San Diego, La Jolla, CA 92093 USA (e-mail: krstic@ucsd.edu).

Color versions of one or more figures in this article are available at https://doi.org/10.1109/TAC.2022.3159292.

Digital Object Identifier 10.1109/TAC.2022.3159292

0018-9286 © 2022 IEEE. Personal use is permitted, but republication/redistribution requires IEEE permission.
See https://www.ieee.org/publications/rights/index.html for more information.

Authorized licensed use limited to: Xiamen University. Downloaded on March 16,2024 at 08:56:11 UTC from IEEE Xplore. Restrictions apply.

However, the abovementioned results only focused on a PDE plant with completely known parameters.

C. Triggered Adaptive Control of PDEs

As in all conventional adaptive control, the previous adaptive control designs for PDEs achieve only asymptotic convergence of the plant states, without a guarantee of exact identification of the unknown parameters. Recently, a new adaptive scheme, using a regulation-triggered batch least-square identifier (BaLSI), was introduced in [21] and [22], which has at least two significant advantages over the traditional adaptive approaches: guaranteeing exponential regulation of the states to zero, as well as finite-time convergence of the estimates to the true values. An application of BaLSI to a two-link manipulator, which is modeled by a highly nonlinear ODE system and subject to four parametric uncertainties, was shown in [4]. Regarding PDEs, this method has been applied in adaptive control of a parabolic PDE [23], and of first-order hyperbolic PDEs in [2], [3], [40], and [42]. However, in the abovementioned designs, the triggering is employed for the parameter estimator (update law), rather than the control law, where the plant states are not sampled. As mentioned in Section I-A, the vibration states may lead to a frequently and fast changing control signal, which is unsuitable in the application of the mining cable elevator, and thus, the vibration states in the control law are required to be sampled as well. Conversely, in [41], an event-triggered adaptive control design was proposed by employing triggering for the control law instead of the parameter estimator, where only asymptotic convergence is achieved. Since the parameter estimator is the more delicate of the two components (the control law and the parameter estimator) of an adaptive control, since it is generally not endowed with convergence guarantees, it is considerably more challenging to employ triggering in the parameter estimator.

In this article, the triggering is employed for updating both the parameter estimator and the plant states in the control law. Both the parameter estimates and the control input thus employ piecewise-constant values. The parameter estimates reach a limit in a finite number of updates, i.e., in finite time and, as a result, exponential regulation of the plant states is achieved. Different from some work in event-triggered control with more than one triggering condition, such as [18] and [35], where distinct triggers are proposed in the sensor-to-controller channels and the controller-to-actuator channels for linear ODE systems, i.e., the triggering times of the triggers are asynchronous, we propose simultaneous triggering of adaptation and feedback in this article.

D. Contributions

1) As compared to the previous results in [12], [14], and [39] on event-triggered backstepping control for 2×2 hyperbolic PDEs with completely known plant parameters, uncertain plant parameters are considered in this article.
2) For the event-triggered adaptive control design of 2×2 hyperbolic PDEs in [41], a continuous parameter update law and event-triggered control inputs are employed, and only asymptotic convergence to zero of the plant states is achieved. This article's event-triggered adaptive control design employs triggering for both the parameter update law and the control input, and achieves finite-time exact identification of the unknown parameters from all but a measure zero set of initial conditions and, as a result of finite-time settling of the parameter estimates, exponential regulation of the plant states to zero.
3) Compared with the triggered-type adaptive control designs for transport PDEs in [2], [3], [40], and [42], where triggering is only employed for the parameter update law rather than the control input, in this article, triggering is employed for updating both the parameter estimator and the plant states in the controller, and both of the parameter estimates and the control input employ piecewise-constant values. Moreover, in-domain couplings between transport PDEs are considered in this article.
4) To the best of authors' knowledge, this is the first adaptive control result, for either PDEs or ODEs, where both the control input and the parameter estimates employ piecewise-constant values.

E. Organization

The problem formulation is shown in Section II. The nominal continuous-in-time control design is presented in Section III. The design of event-triggered control with piecewise-constant parameter identification is proposed in Section IV. The main results including the absence of a Zeno phenomenon, parameter convergence, and exponential regulation of the states are proved in Section V. The effectiveness of the proposed design is illustrated with an application in axial vibration control of a mining cable elevator in Section VI. Finally, Section VII concludes this article.

F. Notation

We adopt the following notation.

1) The symbol $\mathbb{Z}^+$ denotes the set of all nonnegative integers, and $\mathbb{R}_+ := [0, +\infty)$, and $\mathbb{R}_- := (-\infty, 0]$.
2) Let $U \subseteq \mathbb{R}^n$ be a set with a nonempty interior, and let $\Omega \subseteq \mathbb{R}$ be a set. By $C^0(U; \Omega)$, we denote the class of continuous mappings on U, which take values in Ω. By $C^k(U; \Omega)$, where $k \geq 1$, we denote the class of continuous functions on U, which have continuous derivatives of order k on U and take values in Ω.
3) We use the notation $L^2(0, 1)$ for the standard space of the equivalence class of square-integrable, measurable functions defined on $(0, 1)$ and $\|f\| = (\int_0^1 f(x)^2 dx)^{\frac{1}{2}} < +\infty$ for $f \in L^2(0, 1)$.
4) We use the notation $\mathbb{N}$ for the set $\{1, 2, \ldots\}$, i.e., the natural numbers without 0.
5) For an $I \subseteq \mathbb{R}_+$, the space $C^0(I; L^2(0, 1))$ is the space of continuous mappings $I \ni t \mapsto u[t] \in L^2(0, 1)$.
6) Let $u : \mathbb{R}_+ \times [0, 1] \to \mathbb{R}$ be given. We use the notation $u[t]$ to denote the profile of u at certain $t \geq 0$, i.e., $(u[t])(x) = u(x, t)$, for all $x \in [0, 1]$.

II. Problem Formulation

We conduct the control design based on the following 2×2 hyperbolic PDE-ODE system:

$$\dot{\zeta}(t) = a\zeta(t) + bw(0, t) \tag{1}$$

Authorized licensed use limited to: Xiamen University. Downloaded on March 16,2024 at 08:56:11 UTC from IEEE Xplore. Restrictions apply.

$$z_t(x,t) = -q_1 z_x(x,t) + d_1 z(x,t) + d_2 w(x,t) \tag{2}$$
$$w_t(x,t) = q_2 w_x(x,t) + d_3 z(x,t) + d_4 w(x,t) \tag{3}$$
$$z(0,t) = c\zeta(t) - pw(0,t) \tag{4}$$
$$w(1,t) = c_0 U(t) \tag{5}$$

for $x \in [0,1], t \in [0,\infty)$, where $\zeta(t)$ is a scalar ODE state and scalar functions $z(x,t)$ and $w(x,t)$ are PDE states. The function $U(t)$ is the control input to be designed. The positive constants q_1, q_2 are transport speeds, and $p \neq 0$, $c_0 \neq 0$ are arbitrary constants. The ODE system parameter a and the coefficients d_2, d_3 of the PDE in-domain couplings are unknown. To make the problem as nontrivial as we can within this class, we only consider the case where the in-domain instability exists, i.e., $d_3 \neq 0$. Other parameters are arbitrary and satisfy Assumptions 1, 2.

Assumption 1: The parameter b is nonzero. For $c \neq 0$, b is not equal to $-\frac{pa}{c}$.

Assumption 2: For $a \neq 0$, the parameters d_1, d_2, d_3, d_4 satisfy

$$q_2 \frac{d_3(\frac{bc}{a}+p)^2 - (d_4-d_1)(\frac{bc}{a}+p) - d_2}{(\frac{bc}{a}+p)(q_1+q_2)} - d_3\left(\frac{bc}{a}+p\right) + d_4 \neq 0.$$

For $a = 0$ and $c = 0$, the parameters d_1, d_2, d_3, d_4 satisfy

$$q_2 \frac{d_3 p^2 - (d_4-d_1)p - d_2}{p(q_1+q_2)} - d_3 p + d_4 \neq 0.$$

For the cases not mentioned in Assumptions 1 and 2, no restrictions are imposed for the corresponding parameters. The generically satisfied Assumptions 1 and 2 act as sufficient (but not necessary) conditions for the parameter convergence of the estimates.

Assumption 3: The bounds of the unknown parameters d_3, d_2, a are known and arbitrary, i.e., $|d_3| \leq \bar{d}_3$, $|d_2| \leq \bar{d}_2$, $|a| \leq \bar{a}$, where $\bar{d}_3, \bar{d}_2, \bar{a}$ are arbitrary positive constants whose values are known.

This work is motivated from the practical issues in the control of mining cable elevators, as mentioned in Section I-A, but the control design and analysis are based on the general model (1)–(5), which covers broader systems, not only the mining cable elevators, but also open-loop unstable systems (both the PDE and ODE subsystems can be open-loop unstable). For example, the control design in this article is also applicable in suppression of vibrations of airplane wings with aeroelastic instability at high Mach numbers [31], [45], which are described by a wave PDE with in-domain fluid pressure represented by positive stiffness and antidamping, i.e., $u_{tt}(x,t) = c_w^2 u_{xx}(x,t) + \mu_w u_t(x,t) + v_w u_x(x,t)$, where $u(x,t)$ denotes the membrane displacements and the physical meanings of the positive coefficients c_w, μ_w, v_w are given in [31]. Applying the Riemann transformations $z(x,t) = u_t(x,t) - c_w u_x(x,t)$, $w(x,t) = u_t(x,t) + c_w u_x(x,t)$, the airplane wing vibration dynamics are transformed to a 2×2 hyperbolic PDE system, covered by the considered plant (1)–(5), where the ODE (5) can describe a mass at the wingtip.

III. Nominal Control Design

We introduce the following backstepping transformation [11]:

$$\alpha(x,t) = z(x,t) - \int_0^x \phi(x,y) z(y,t) dy - \int_0^x \varphi(x,y) w(y,t) dy - \gamma(x)\zeta(t) \tag{6}$$

$$\beta(x,t) = w(x,t) - \int_0^x \Psi(x,y) z(y,t) dy - \int_0^x \Phi(x,y) w(y,t) dy - \lambda(x)\zeta(t) \tag{7}$$

and its inverse

$$z(x,t) = \alpha(x,t) - \int_0^x \bar{\phi}(x,y)\alpha(y,t) dy - \int_0^x \bar{\varphi}(x,y)\beta(y,t) dy - \bar{\gamma}(x)\zeta(t) \tag{8}$$

$$w(x,t) = \beta(x,t) - \int_0^x \bar{\Psi}(x,y)\alpha(y,t) dy - \int_0^x \bar{\Phi}(x,y)\beta(y,t) dy - \bar{\lambda}(x)\zeta(t) \tag{9}$$

to convert the plant (1)–(5) to the target system

$$\dot{\zeta}(t) = -a_{\rm m}\zeta(t) + b\beta(0,t) \tag{10}$$
$$\alpha(0,t) = -p\beta(0,t) \tag{11}$$
$$\alpha_t(x,t) = -q_1\alpha_x(x,t) + d_1\alpha(x,t) \tag{12}$$
$$\beta_t(x,t) = q_2\beta_x(x,t) + d_4\beta(x,t) \tag{13}$$
$$\beta(1,t) = 0 \tag{14}$$

where $a_{\rm m} = b\kappa - a > 0$ is ensured by a design parameter κ satisfying

$$\kappa > \frac{\bar{a}}{b}, \quad \forall b > 0, \qquad \kappa < \frac{\bar{a}}{b}, \qquad \forall b < 0. \tag{15}$$

The conditions on the kernels $\phi(x,y)$, $\varphi(x,y)$, $\gamma(x)$, $\Psi(x,y)$, $\Phi(x,y)$, $\lambda(x)$ and $\bar{\phi}(x,y)$, $\bar{\varphi}(x,y)$, $\bar{\gamma}(x)$, $\bar{\Psi}(x,y)$, $\bar{\Phi}(x,y)$, $\bar{\lambda}(x)$ in the backstepping transformations (6)–(9), which are obtained by matching the original system (1)–(5) and the target system (10)–(14), are shown in Appendix A, and the well-posedness has been proved in [11, Th. 4.1]. The nominal continuous-in-time control is obtained from the right boundary condition (14) in the target system as follows:

$$U(t) = \frac{1}{c_0}\int_0^1 \Psi(1,y;\theta) z(y,t) dy + \frac{1}{c_0}\int_0^1 \Phi(1,y;\theta) w(y,t) dy + \frac{1}{c_0}\lambda(1;\theta)\zeta(t). \tag{16}$$

Writing $\theta = [d_3, d_2, a]^T$ after ";" in $\Psi(x,y;\theta)$, $\Phi(x,y;\theta)$, and $\lambda(x;\theta)$ emphasizes the fact that $\Psi(x,y)$, $\Phi(x,y)$, $\lambda(x)$ depend on the unknown parameters d_3, d_2, a, due to the fact that Ψ, Φ, λ is the solution of the kernel PDE set, shown in Appendix A, with the unknown coefficients d_3, d_2, a.

IV. Event-Triggered Control Design with Piecewise-Constant Parameter Identification

Based on the nominal continuous-in-time feedback (16), we give the form of an adaptive event-triggered control law U_d, as follows:

$$U_d(t) = \frac{1}{c_0}\int_0^1 \Psi(1,y;\hat{\theta}(t_i)) z(y,t_i) dy + \frac{1}{c_0}\int_0^1 \Phi(1,y;\hat{\theta}(t_i)) w(y,t_i) dy + \frac{1}{c_0}\lambda(1;\hat{\theta}(t_i))\zeta(t_i) \tag{17}$$

Authorized licensed use limited to: Xiamen University. Downloaded on March 16,2024 at 08:56:11 UTC from IEEE Xplore. Restrictions apply.

for $t \in [t_i, t_{i+1})$, where $\hat{\theta} = [\hat{d}_3, \hat{d}_2, \hat{a}]^T$ is an estimate, generated with a triggered batch least-squares identifier, of the three unknown parameters d_3, d_2, a. The identifier is presented shortly, and $\{t_i \geq 0\}_{i=0}^{\infty}$, $i \in \mathbb{Z}^+$, is the sequence of time instants, which, along with the parameter estimates and sampled states in (17), is defined in the following section.

When we mention the continuous-in-state control input U_c, we refer to the control input consisting of triggered parameter estimates and continuous states, i.e.,

$$U_c(t) = \frac{1}{c_0}\int_0^1 \Psi(1, y; \hat{\theta}(t_i)) z(y,t)dy + \frac{1}{c_0}\int_0^1 \Phi(1, y; \hat{\theta}(t_i)) w(y,t)dy + \frac{1}{c_0}\lambda(1; \hat{\theta}(t_i))\zeta(t) \quad (18)$$

for $t \in [t_i, t_{i+1})$. Define the difference between the continuous-in-state control input U_c in (18) and the event-triggered control input U_d in (17) as $d(t)$, given by

$$\begin{aligned} d(t) &= U_c(t) - U_d(t) \\ &= \frac{1}{c_0}\int_0^1 \Psi(1, y; \hat{\theta}(t_i))(z(y,t) - z(y,t_i))dy \\ &\quad + \frac{1}{c_0}\int_0^1 \Phi(1, y; \hat{\theta}(t_i))(w(y,t) - w(y,t_i))dy \\ &\quad + \frac{1}{c_0}\lambda(1; \hat{\theta}(t_i))(\zeta(t) - \zeta(t_i)), \quad t \in [t_i, t_{i+1}) \end{aligned} \quad (19)$$

which reflects the deviation of the plant states from their sampled values. Define the difference between the continuous-in-state control input $U_c(t)$ in (18) and the nominal continuous-in-time control input $U(t)$ in (16) as $\xi(t)$, given by

$$\begin{aligned} \xi(t) &= U(t) - U_c(t) \\ &= \frac{1}{c_0}\int_0^1 (\Psi(1, y; \theta) - \Psi(1, y; \hat{\theta}(t_i))) z(y,t)dy \\ &\quad + \frac{1}{c_0}\int_0^1 (\Phi(1, y; \theta) - \Phi(1, y; \hat{\theta}(t_i))) w(y,t)dy \\ &\quad + \frac{1}{c_0}(\lambda(1; \theta) - \lambda(1; \hat{\theta}(t_i)))\zeta(t), \quad t \in [t_i, t_{i+1}) \end{aligned} \quad (20)$$

which reflects the deviation of the estimates from the actual unknown parameters. The deviations $d(t)$ and $\xi(t)$ will be used in the following design and analysis.

A. Triggering Mechanism

Before showing the triggering mechanism that determines the sequence of time instants $\{t_i \geq 0\}_{i=0}^{\infty}$, $i \in \mathbb{Z}^+$, we introduce the two sets S_i and $\bar{S}_i$, which will be used in the triggering mechanism to judge whether the exact identification of the unknown parameters has been achieved. The set S_i is defined as

$$S_i := \Big\{\bar{\ell} = (\ell_1, \ell_2)^T \in \Theta_1 : \bar{Z}_n(\mu_{i+1}, t_{i+1}) = \bar{G}_n(\mu_{i+1}, t_{i+1})\bar{\ell}, \; n = 1, 2, \dots, \Big\}, \quad i \in \mathbb{Z}^+ \quad (21)$$

where $\Theta_1 = \{\bar{\ell} \in \mathbb{R}^2 : |\ell_1| \leq \bar{d}_3, |\ell_2| \leq \bar{d}_2\}$, and $\bar{Z}_n, \bar{G}_n$ associated with the plant states over a time interval $[\mu_{i+1}, t_{i+1}]$ (the time instant μ_{i+1} is defined shortly) are

$$\bar{Z}_n(\mu_{i+1}, t_{i+1}) = [H_{n,1}(\mu_{i+1}, t_{i+1}), H_{n,2}(\mu_{i+1}, t_{i+1})]^T \quad (22)$$

$$\bar{G}_n(\mu_{i+1}, t_{i+1}) = \begin{bmatrix} Q_{n,1}(\mu_{i+1}, t_{i+1}) & Q_{n,2}(\mu_{i+1}, t_{i+1}) \\ Q_{n,2}(\mu_{i+1}, t_{i+1}) & Q_{n,3}(\mu_{i+1}, t_{i+1}) \end{bmatrix} \quad (23)$$

with

$$H_{n,1}(\mu_{i+1}, t_{i+1}) = \int_{\mu_{i+1}}^{t_{i+1}} g_{n,1}(t, \mu_{i+1}) f_n(t, \mu_{i+1}) dt \quad (24)$$

$$H_{n,2}(\mu_{i+1}, t_{i+1}) = \int_{\mu_{i+1}}^{t_{i+1}} g_{n,2}(t, \mu_{i+1}) f_n(t, \mu_{i+1}) dt \quad (25)$$

$$Q_{n,1}(\mu_{i+1}, t_{i+1}) = \int_{\mu_{i+1}}^{t_{i+1}} g_{n,1}(t, \mu_{i+1})^2 dt \quad (26)$$

$$Q_{n,2}(\mu_{i+1}, t_{i+1}) = \int_{\mu_{i+1}}^{t_{i+1}} g_{n,1}(t, \mu_{i+1}) g_{n,2}(t, \mu_{i+1}) dt \quad (27)$$

$$Q_{n,3}(\mu_{i+1}, t_{i+1}) = \int_{\mu_{i+1}}^{t_{i+1}} g_{n,2}(t, \mu_{i+1})^2 dt \quad (28)$$

where

$$\begin{aligned} f_n(t, \mu_{i+1}) &= \int_0^1 \sin(x\pi n) z(x,t)dx + \int_0^1 \sin(x\pi n) w(x,t)dx \\ &\quad - \int_0^1 \sin(x\pi n) z(x, \mu_{i+1})dx - \int_0^1 \sin(x\pi n) w(x, \mu_{i+1})dx \\ &\quad - \pi n \int_{\mu_{i+1}}^t \int_0^1 \cos(x\pi n)(q_1 z(x,\tau) - q_2 w(x,\tau)) dx d\tau \\ &\quad - \int_{\mu_{i+1}}^t \int_0^1 \sin(x\pi n)(d_1 z(x,\tau) + d_4 w(x,\tau)) dx d\tau \end{aligned} \quad (29)$$

$$g_{n,1}(t, \mu_{i+1}) = \int_{\mu_{i+1}}^t \int_0^1 \sin(x\pi n) z(x,\tau) dx d\tau \quad (30)$$

$$g_{n,2}(t, \mu_{i+1}) = \int_{\mu_{i+1}}^t \int_0^1 \sin(x\pi n) w(x,\tau) dx d\tau \quad (31)$$

for $n = 1, 2, \ldots$. The set $\bar{S}_i$ is defined as

$$\bar{S}_i := \Big\{\ell_3 \in [-\bar{a}, \bar{a}] : H_3(\mu_{i+1}, t_{i+1}) = Q_4(\mu_{i+1}, t_{i+1})\ell_3, \Big\}, i \in \mathbb{Z}^+ \quad (32)$$

where the function H_3 is defined as

$$H_3(\mu_{i+1}, t_{i+1}) = \int_{\mu_{i+1}}^{t_{i+1}} g_a(t, \mu_{i+1}) f_a(t, \mu_{i+1}) dt \quad (33)$$

and the function Q_4 is defined as

$$Q_4(\mu_{i+1}, t_{i+1}) = \int_{\mu_{i+1}}^{t_{i+1}} g_a(t, \mu_{i+1})^2 dt \quad (34)$$

for $i \in \mathbb{Z}^+$, with

$$f_a(t, \mu_{i+1}) = \zeta(t) - \zeta(\mu_{i+1}) - b\int_{\mu_{i+1}}^t w(0,\tau)d\tau \quad (35)$$

$$g_a(t, \mu_{i+1}) = \int_{\mu_{i+1}}^t \zeta(\tau)d\tau. \quad (36)$$

Based on the abovementioned definitions, we introduce the triggering mechanism next. The sequence of time instants $\{t_i \geq 0\}_{i=0}^{\infty}$ ($t_0 = 0$) is defined as

$$t_{i+1} = \min\{\tau_i, r_i\} \quad (37)$$

Authorized licensed use limited to: Xiamen University. Downloaded on March 16,2024 at 08:56:11 UTC from IEEE Xplore. Restrictions apply.

where τ_i is given by

$$\tau_i = \inf\{t > t_i : d(t)^2 \geq \vartheta V(t) - m(t)\} \tag{38}$$

and the functions $V(t), m(t)$ will be defined later, and where r_i is defined next. If $i \geq 1$ and there exists a singleton S_j for a certain j ($j \in \mathbb{Z}^+$, $j \leq i-1$) and a singleton $\bar{S}_k$ for a certain k ($k \in \mathbb{Z}^+$, $k \leq i-1$), then r_i is set as

$$r_i := +\infty \tag{39}$$

or else, r_i is set as

$$r_i = \max\{t_i + \underline{r}, \min\{\inf\{t > t_i : \Omega(t) = (1+\delta)\Omega(t_i)\}, t_i + T\}\}, \quad \Omega(t_i) \neq 0 \tag{40}$$

$$r_i = t_i + T, \quad \Omega(t_i) = 0 \tag{41}$$

where the design parameters δ, T are positive and free, and $\underline{r}$ is a positive constant satisfying

$$0 < \underline{r} < T \tag{42}$$

and where the function $\Omega(t)$ is defined as

$$\Omega(t) = \|z[t]\|^2 + \|w[t]\|^2 + \zeta(t)^2. \tag{43}$$

The Lyapunov function $V(t)$ in (38) is given as

$$V(t) = \frac{1}{2}\zeta(t)^2 + \frac{1}{2}r_a\int_0^1 e^{\delta_1 x}\beta(x,t)^2 dx + \frac{1}{2}\int_0^1 e^{-\delta_2 x}\alpha(x,t)^2 dx \tag{44}$$

where the positive constants r_a, δ_1, δ_2, which are design parameters, are chosen to satisfy

$$\delta_1 > \frac{2|d_4|}{q_2},\ \delta_2 > \frac{2|d_1|}{q_1},\ r_a > \frac{b^2}{q_2(b\kappa - \bar{a})} + \frac{p^2 q_1}{q_2} \tag{45}$$

which depend only on the design parameter κ in (15), the known plant parameters and the known bounds of the unknown parameters in Assumption 3.

The internal dynamic variable $m(t)$ in (38) satisfies the ordinary differential equation

$$\dot{m}(t) = -\eta m(t) + \lambda_d d(t)^2 - \sigma V(t) - \kappa_1\alpha(1,t)^2 - \kappa_2\beta(0,t)^2 \tag{46}$$

with the initial condition $m(0) < 0$. Choose the positive design parameters κ_1, κ_2 in (46) to satisfy

$$\kappa_1 \geq 2\max\{\lambda_a, \lambda_\alpha\},\ \kappa_2 \geq 2\max\{\lambda_a, \lambda_\beta\} \tag{47}$$

where the positive constants λ_α, λ_β, λ_a are

$$\lambda_\alpha = \frac{1}{2}q_1 e^{-\delta_2},\ \ \lambda_\beta = \frac{1}{2}q_2 r_a + \frac{1}{2}|b| \tag{48}$$

$$\lambda_a = \frac{6}{c_0^2}\max_{y\in[0,1],\theta_1\in\Theta,\theta_2\in\Theta}\left\{|M_1(y,\theta_1,\theta_2)|^2, |M_2(y,\theta_1,\theta_2)|^2, |M_3(\theta_1,\theta_2)|^2, |M_4(\theta_1,\theta_2)|^2, |M_5(\theta_1,\theta_2)|^2, |M_6(\theta_1,\theta_2)|^2\right\}. \tag{49}$$

The functions $M_1,\ldots,M_6$ are given in Appendix B, and λ_a depends only on the design parameter κ, the known plant parameters, and the known bounds of the unknown parameters in Assumption 3. Choose the design parameters λ_d, σ, η in (46) such that they satisfy

$$\lambda_d \geq \frac{1}{\mu}q_2 r_a e^{\delta_1}c_0^2 \tag{50}$$

$$0 < \sigma < \frac{\nu_a}{\mu},\ \eta > \nu_a - \mu\sigma \tag{51}$$

where the positive constants μ, ν_a are

$$\mu \leq \min\left\{\frac{q_2 r_a}{2\kappa_2} - \frac{b^2}{2\kappa_2(b\kappa - \bar{a})} - \frac{p^2 q_1}{2\kappa_2}, \frac{1}{2\kappa_1}q_1 e^{-\delta_2}\right\} \tag{52}$$

$$\nu_a = \frac{1}{\xi_2}\min\left\{\frac{1}{2}(b\kappa - \bar{a}), \frac{1}{2}\delta_1 q_2 r_a - r_a|d_4|, \left(\frac{1}{2}\delta_2 q_1 - |d_1|\right)e^{-\delta_2}\right\} \tag{53}$$

with

$$\xi_2 = \frac{1}{2}\min\{1, r_a e^{\delta_1}\} > 0. \tag{54}$$

The final design parameter ϑ in (38) is chosen in accordance with the following condition:

$$0 < \vartheta \leq \max\left\{1, \frac{\sigma}{\lambda_d}\right\}. \tag{55}$$

The time instant μ_{i+1} used in (21) and (32) is defined as

$$\mu_{i+1} := \min\{t_f : f \in \{0,\ldots,i\}, t_f \geq t_{i+1} - \tilde{N}T\} \tag{56}$$

according to [22], where the positive integer $\tilde{N} \geq 1$ is a design parameter, and the positive constant T is the maximum dwell time according to (37)–(41). The flowchart of implementing the designed triggering mechanism (37)–(41) is shown in Fig. 1, and the proof of the fact that the triggering mechanism (37)–(41) is well-defined and produces an increasing sequence of events will be shown in Lemma 3.

Design rationale of the triggering mechanism (37)–(41): According to (19) and (20), i.e., two deviation signals affecting the stability obtained under the nominal continuous-in-time control, we know the size of $d(t)$ is associated with the deviation of the plant states from their sampled values, and the size of $\xi(t)$ is associated with the deviation of the parameter estimates from the actual unknown parameters. According to the form of the event trigger presented in [14], the triggering condition (38) is designed, based on the evolution of the square of $d(t)$, to guarantee that $d(t)^2$ is bounded by the plant norm, and an internal dynamic variable $m(t)$ defined in (46) (the introduction of $m(t)$ is to ensure that no Zeno phenomenon occurs, as will be seen in Claim 2 in Lemma 3). Even if $d(t)$ is ensured to be small enough in the closed-loop system, a large growth of the plant norm still may appear under a large $\xi(t)$ (as the analysis in the proof of property 3) of Theorem 1). Therefore, in addition to the triggering condition (38) designed to bound $d(t)$, another triggering condition in (40) is designed based on evaluating the growth of the plant norm [22], where the updates are triggered if the plant norm has grown by a certain factor, to avoid a large overshoot. Introducing the design parameters $\underline{r}$, T in (40) and (41), which set the lower and upper bounds of the interval between r_i, enables the user to adjust the number of r_i. As will be seen latter, the condition below (38), that there exist the singletons sets S_j, $\bar{S}_k$, implies that the exact identification of θ has been achieved at t_i, for $i \geq 1$. Therefore, in this case, we set $r_i := +\infty$ in (39), in order to avoid unnecessary updates of the control signal after the exact parameter identification has been achieved (when initial estimates are not the true values).

The first triggering condition (38) is for resampling the states $z[t], w[t], \zeta(t)$, and the second triggering condition (40), (41) is for recomputing the estimate $\hat{\theta}(t)$. The synchronous triggering is ensured by the fact that, if either condition is met, both recomputing of $\hat{\theta}(t)$ and resampling of $z[t], w[t], \zeta(t)$

Authorized licensed use limited to: Xiamen University. Downloaded on March 16,2024 at 08:56:11 UTC from IEEE Xplore. Restrictions apply.

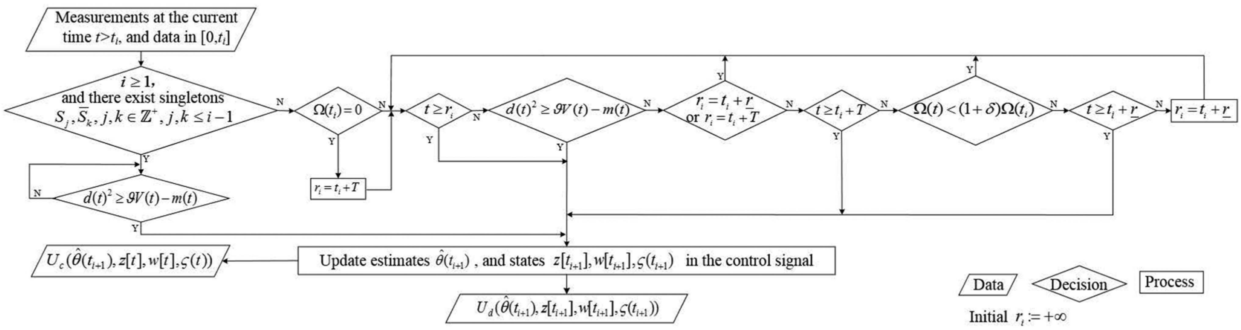

Fig. 1. Flowchart of implementing the triggering mechanism (37)–(41).

are done simultaneously, due to (37). All design parameters are $\kappa, \underline{r}, \delta_1, \delta_2, r_a, \kappa_1, \kappa_2, \lambda_d, \sigma, \eta, \vartheta$, whose conditions are cascaded rather than mutually dependent, and defined only by known parameters. They can be solved in the sequence (15), (42), (45), (47), (50), (51), (55). The motivation for defining these conditions of the design parameters will become clear in the rest of this article.

B. Least-Squares Identifier

According to (2) and (3), we get for $\tau>0$ and $n=1,2,\ldots$ that

$$\begin{aligned}&\frac{d}{d\tau}\left(\int_0^1 \sin(x\pi n)z(x,\tau)dx+\int_0^1 \sin(x\pi n)w(x,\tau)dx\right)\\ =&-q_2\pi n\int_0^1\cos(x\pi n)w(x,\tau)dx\\ &+d_1\int_0^1 \sin(x\pi n)z(x,\tau)dx+d_2\int_0^1 \sin(x\pi n)w(x,\tau)dx\\ &+q_1\pi n\int_0^1\cos(x\pi n)z(x,\tau)dx\\ &+d_3\int_0^1 \sin(x\pi n)z(x,\tau)dx+d_4\int_0^1 \sin(x\pi n)w(x,\tau)dx.\end{aligned}\tag{57}$$

Integrating (57), (1) from μ_{i+1} to t, yields

$$f_n(t,\mu_{i+1})=d_3g_{n,1}(t,\mu_{i+1})+d_2g_{n,2}(t,\mu_{i+1})\tag{58}$$
$$f_a(t,\mu_{i+1})=ag_a(t,\mu_{i+1})\tag{59}$$

where $f_n, g_{n,1}, g_{n,2}$ are given in (29)–(31), and f_a, g_a are defined in (35) and (36).

Define the function $h_{i,n}:\mathbb{R}^3\to\mathbb{R}_+$ by the formula

$$\begin{aligned}h_{i,n}(\ell)=&\int_{\mu_{i+1}}^{t_{i+1}}\big[(f_n(t,\mu_{i+1})\\ &-\ell_1g_{n,1}(t,\mu_{i+1})-\ell_2g_{n,2}(t,\mu_{i+1}))^2\\ &+(f_a(t,\mu_{i+1})-\ell_3g_a(t,\mu_{i+1}))^2\big]dt,\ i\in\mathbb{Z}^+\end{aligned}\tag{60}$$

for $n=1,2,\ldots$, $\ell=[\ell_1,\ell_2,\ell_3]^T$.

According to (58) and (59), the function $h_{i,n}(\ell)$ in (60) has a global minimum $h_{i,n}(\theta)=0$. We get from the Fermat's theorem (vanishing gradient at extrema) that the following matrix equation holds for every $i\in\mathbb{Z}^+$ and $n=1,2,\ldots$

$$Z_n(\mu_{i+1},t_{i+1})=G_n(\mu_{i+1},t_{i+1})\theta\tag{61}$$

where

$$Z_n=[H_{n,1},H_{n,2},H_3]^T,\quad G_n=\begin{bmatrix}Q_{n,1}&Q_{n,2}&0\\ Q_{n,2}&Q_{n,3}&0\\ 0&0&Q_4\end{bmatrix}\tag{62}$$

and $H_{n,1}(\mu_{i+1},t_{i+1})$, $H_{n,2}(\mu_{i+1},t_{i+1})$, $H_3(\mu_{i+1},t_{i+1})$, $Q_{n,1}(\mu_{i+1},t_{i+1})$, $Q_{n,2}(\mu_{i+1},t_{i+1})$, $Q_{n,3}(\mu_{i+1},t_{i+1})$, $Q_4(\mu_{i+1},t_{i+1})$ are given in (24)–(28), (33), (34). Indeed, (61), (62) are obtained by differentiating the functions $h_{i,n}(\ell)$ defined by (60) with respect to ℓ_1, ℓ_2, ℓ_3, respectively, and evaluating the derivatives at the position of the global minimum $(\ell_1,\ell_2,\ell_3)=(d_3,d_2,a)$.

The parameter estimator (update law) is defined as

$$\begin{aligned}\hat{\theta}(t_{i+1})=\operatorname{argmin}\Big\{&\left|\ell-\hat{\theta}(t_i)\right|^2:\ell\in\Theta,\\ &Z_n(\mu_{i+1},t_{i+1})=G_n(\mu_{i+1},t_{i+1})\ell,\ \ n=1,2,\ldots\Big\}\end{aligned}\tag{63}$$

where $\Theta=\{\ell\in\mathbb{R}^3:|\ell_1|\leq\bar{d}_3,|\ell_2|\leq\bar{d}_2,|\ell_3|\leq\bar{a}\}$.

Proposition 1: For every $(z[t_i],w[t_i])^T\in L^2((0,1);\mathbb{R}^2)$, $\zeta(t_i)\in\mathbb{R}$, $m(t_i)\in\mathbb{R}_-$, and $\hat{\theta}(t_i)\in\Theta$, there exists a unique (weak) solution $((z,w)^T,\zeta)\in C^0([t_i,t_{i+1}];L^2(0,1);\mathbb{R}^2)\times C^0([t_i,t_{i+1}];\mathbb{R})$, $m\in C^0([t_i,t_{i+1}];\mathbb{R}^-)$ to the system (1)–(5), (17), (46), and $\hat{\theta}\in\Theta$ in (63), between two time instants t_i,t_{i+1}.

Proof: The proof is similar to that of Proposition 1 in [40], and thus, it is omitted. ∎

V. Main Result

Theorem 1: For all initial data $(z[0],w[0])^T\in C^1([0,1])$, $\zeta(0)\in\mathbb{R}$, $\hat{\theta}(0)\in\Theta$, $m(0)<0$, the closed-loop system (1)–(5) under the controller (17), with the triggering mechanism (37)–(41), and the least-squares identifier defined by (63) has the following properties.

1) No Zeno phenomenon occurs, i.e., $\lim_{i\to\infty}t_i=+\infty$, and the closed-loop system is well-posed.

2) If the finite-time convergence of parameter estimates to the true values is not achieved, it implies $\Omega(t)\equiv 0$ on $t\in[\frac{1}{q_1},\infty)$ and $m(t)$ is exponentially convergent to zero. If the parameter estimate $\hat{\theta}(t)$ reaches the true value θ in finite time, i.e.,

$$\hat{\theta}(t)=\theta\qquad\forall t\geq t_\varepsilon\tag{64}$$

for certain $\varepsilon\in\mathbb{Z}^+$, then $t_\varepsilon\leq\frac{1}{q_1}+\frac{1}{q_2}+T$.

3) If the finite-time convergence of parameter estimates to the true values is achieved, the exponential regulation of the closed-loop system is obtained in the sense that there exist positive

Authorized licensed use limited to: Xiamen University. Downloaded on March 16,2024 at 08:56:11 UTC from IEEE Xplore. Restrictions apply.

constants M, λ_1 such that

$$\bar{\Omega}(t) \leq M\bar{\Omega}(0)e^{-\lambda_1 t}, \quad t \geq 0 \tag{65}$$

where

$$\bar{\Omega}(t) = \|z[t]\|^2 + \|w[t]\|^2 + \zeta(t)^2 + |m(t)| \tag{66}$$

and where M is related to the initial estimate $\hat{\theta}(0)$.

The proof of Theorem 1 is based on the following technical lemmas. First, we present the two lemmas that will be used in the analysis of minimal dwell time.

Lemma 1: For $d(t)$ defined in (19), there exists a positive constant λ_a such that

$$\dot{d}(t)^2 \leq \lambda_a \bigg(d(t)^2 + \alpha(1,t)^2 + \beta(0,t)^2 + \|\alpha(\cdot,t)\|^2 + \|\beta(\cdot,t)\|^2 + \zeta(t)^2 \bigg) \tag{67}$$

for $t \in (t_i, t_{i+1})$, where the positive constant λ_a is given in (49), which depends only on the design parameter κ in (15), the known plant parameters, and the known bounds $\bar{a}, \bar{d}_3, \bar{d}_2$ of the unknown parameters.

Proof: Inserting $U_d(t)$ into (5), we have

$$w(1,t) = c_0 U_d(t). \tag{68}$$

Applying (19), (20), it allows us to rewrite (68) as

$$w(1,t) = c_0(U_c(t) - d(t)) = c_0 U(t) - c_0\xi(t) - c_0 d(t). \tag{69}$$

Inserting (8), (9) into (20), we obtain

$$\xi(t) = \frac{1}{c_0}\left[\int_0^1 \tilde{K}_1(y;\hat{\theta}(t_i),\theta)\alpha(y,t)dy + \int_0^1 \tilde{K}_2(y;\hat{\theta}(t_i),\theta)\beta(y,t)dy + \tilde{K}_3(\hat{\theta}(t_i),\theta)\zeta(t)\right] \tag{70}$$

for $t \in [t_i, t_{i+1})$, where the functions $\tilde{K}_1, \tilde{K}_2, \tilde{K}_3$ are shown in Appendix B. Applying the backstepping control design in Section III into (1)–(4), (69), the right boundary condition of the target system (10)–(14) becomes

$$\beta(1,t) = -c_0\xi(t) - c_0 d(t). \tag{71}$$

Inserting the inverse backstepping transformations into $U_c(t)$ in (18) to replace the original states by the states in the target system, we obtain

$$U_c(t) = \frac{1}{c_0}\int_0^1 K_1(y,\hat{\theta}(t_i),\theta)\alpha(y,t)dy + \frac{1}{c_0}\int_0^1 K_2(y,\hat{\theta}(t_i),\theta)\beta(y,t)dy + \frac{1}{c_0}K_3(\hat{\theta}(t_i),\theta)\zeta(t) \tag{72}$$

for $t \in [t_i, t_{i+1})$, where the functions K_1, K_2, K_3 are shown in Appendix B. The event-triggered control input U_d is constant on $t \in (t_i, t_{i+1})$, i.e., $\dot{U}_d(t) = 0$. Taking the time derivative of (19), recalling (70), (71), (72), we obtain

$$\begin{aligned}\dot{d}(t) = \dot{U}_c(t) = \frac{1}{c_0}\bigg[&\int_0^1 M_1(y,\hat{\theta}(t_i),\theta)\alpha(y,t)dy \\ &- \int_0^1 M_2(y,\hat{\theta}(t_i),\theta)\beta(y,t)dy - M_3(\hat{\theta}(t_i),\theta)\zeta(t) \\ &+ M_4(\hat{\theta}(t_i),\theta)\beta(0,t) - M_5(\hat{\theta}(t_i),\theta)\alpha(1,t) \\ &- M_6(\hat{\theta}(t_i),\theta)d(t)\bigg]\end{aligned} \tag{73}$$

where the functions $M_1,\ldots,M_6$ are shown in Appendix B. Applying the Cauchy–Schwarz inequality into (73), we obtain (67). ■

Lemma 2: For the internal dynamic variable $m(t)$ defined in (46), it holds that $m(t) < 0$.

Proof: According to (38), events are triggered to guarantee that $d(t)^2 \leq \vartheta V(t) - m(t)$. Recalling (46), we then have

$$\begin{aligned}\dot{m}(t) \leq& -(\eta+\lambda_d)m(t) + (\lambda_d\vartheta - \sigma)V(t) \\ &- \kappa_1\alpha(1,t)^2 - \kappa_2\beta(0,t)^2 \\ \leq& -(\eta+\lambda_d)m(t), \quad t \geq 0\end{aligned} \tag{74}$$

where $\vartheta \leq \frac{\sigma}{\lambda_d}$ obtained from (55) has been used. Together with $m(0) < 0$, we conclude that $m(t) < 0$. ■

Relying on Lemmas 1, 2, we present the following lemma, which shows that the event trigger is well-defined and produces an increasing sequence of events.

Lemma 3: Under the triggering mechanism defined by (37)–(41), the minimal dwell time exists, in the sense of $t_{i+1} - t_i \geq \min\{\underline{\tau}, \underline{r}\} > 0, \forall i \in \mathbb{Z}^+$ for some positive $\underline{\tau}$.

Proof: At a time instant t_i, the next time instant t_{i+1} is triggered by either r_i in (40), (41) or τ_i in (38). Next, we present two claims regarding the minimal dwell time in the two situations that t_{i+1} is triggered by either r_i or τ_i, respectively.

Claim 1: For an arbitrary time instant t_i, if the next time instant t_{i+1} is triggered by r_i in (41) and (40), then $t_{i+1} - t_i \geq \underline{r} > 0$.

Proof: If $\Omega(t_i) \neq 0$, the interval $t_{i+1} - t_i$ is greater than $\underline{r} > 0$ by virtue of (40). If $\Omega(t_i) = 0$, according to (41), the interval $t_{i+1} - t_i$ is equal to the positive constant T, which is larger than $\underline{r}$ according to (42). ■

Claim 2: For an arbitrary time instant t_i, if the next time instant t_{i+1} is triggered by τ_i in (38), there exists a minimal dwell time $\underline{\tau} > 0$ such that $t_{i+1} - t_i \geq \underline{\tau}$.

Proof: We know from (38) that the events are triggered to guarantee $d(t)^2 \leq \vartheta V(t) - m(t)$ for all $t \geq 0$. Introduce the following function $\psi(t)$:

$$\psi(t) = \frac{d(t)^2 + \frac{1}{2}m(t)}{\vartheta V(t) - \frac{1}{2}m(t)} \tag{75}$$

which was proposed in [14]. We have that $\psi(t_{i+1}) = 1$ because the event is triggered, and that $\psi(t_i) < 0$ because of $m(t) < 0$ proved in Lemma 2 and $d(t_i) = 0$ according to (19). The function $\psi(t)$ is a continuous function on $[t_i, t_{i+1}]$ recalling Proposition 1. By the intermediate value theorem, there exists $t^* > t_i$ such that $\psi(t) \in [0,1]$ when $t \in [t^*, t_{i+1}]$. The minimal dwell time can be found as the minimal time it takes for $\psi(t)$ from 0 to 1. Defining

$$\Omega_0(t) = \|\alpha(\cdot,t)\|^2 + \|\beta(\cdot,t)\|^2 + \zeta(t)^2 \tag{76}$$

recalling (44), the following inequality holds:

$$\xi_1\Omega_0(t) \leq V(t) \leq \xi_2\Omega_0(t) \tag{77}$$

where the positive constant ξ_1 is $\xi_1 = \min\{\frac{1}{2}, \frac{1}{2}r_a, \frac{1}{2}e^{-\delta_2}\}$ and the positive constant ξ_2 is defined in (54). Taking the time derivative of $V(t)$ in (44) and applying (10)–(13), using integration by parts, we obtain

$$\dot{V}(t) = -a_{\mathrm{m}}\zeta(t)^2 + \zeta(t)b\beta(0,t) + \frac{1}{2}q_2 r_a e^{\delta_1}\beta(1,t)^2 - \frac{1}{2}\delta_1 q_2 r_a\int_0^1 e^{\delta_1 x}\beta(x,t)^2 dx + r_a d_4\int_0^1 e^{\delta_1 x}\beta(x,t)^2 dx$$

Authorized licensed use limited to: Xiamen University. Downloaded on March 16,2024 at 08:56:11 UTC from IEEE Xplore. Restrictions apply.

$$- \frac{1}{2}q_1 e^{-\delta_2}\alpha(1,t)^2 + \frac{1}{2}q_1\alpha(0,t)^2 - \frac{1}{2}q_2 r_a\beta(0,t)^2$$
$$- \frac{1}{2}\delta_2 q_1 \int_0^1 e^{-\delta_2 x}\alpha(x,t)^2 dx + d_1 \int_0^1 e^{-\delta_2 x}\alpha(x,t)^2 dx. \tag{78}$$

We then have

$$\dot{V}(t) \geq -\mu_0 V - \lambda_\alpha \alpha(1,t)^2 - \lambda_\beta \beta(0,t)^2 \tag{79}$$

where the positive constant μ_0 is

$$\mu_0 = \frac{1}{\xi_1}\max\left\{\frac{1}{2}\delta_1 q_2 r_a e^{\delta_1} + r_a|d_4|e^{\delta_1}, \frac{1}{2}\delta_2 q_1 + |d_1|, a_{\rm m} + \frac{1}{2}|b|\right\} \tag{80}$$

and $\lambda_\alpha, \lambda_\beta$ are given in (48).

Taking the derivative of (75) for all $t \in (t^*, t_{i+1})$, applying Young's inequality, using (67) in Lemma 1, inserting (46), (79), and applying (76), (77) to rewrite $\|\alpha(\cdot,t)\|^2 + \|\beta(\cdot,t)\|^2 + \zeta(t)^2$, we have

$$\begin{aligned}
\dot{\psi} &= \frac{2d(t)\dot{d}(t) + \frac{1}{2}\dot{m}(t)}{\vartheta V(t) - \frac{1}{2}m(t)} - \frac{(\vartheta \dot{V}(t) - \frac{1}{2}\dot{m}(t))}{\vartheta V(t) - \frac{1}{2}m(t)}\psi \\
&\leq \frac{1}{\vartheta V(t) - \frac{1}{2}m(t)}\Bigg[\left(\lambda_a + 1 + \frac{1}{2}\lambda_d\right)d(t)^2 \\
&\quad + \left(\lambda_a - \frac{\kappa_1}{2}\right)\alpha(1,t)^2 \\
&\quad + \left(\lambda_a - \frac{1}{2}\kappa_2\right)\beta(0,t)^2 + \frac{\lambda_a}{\xi_1}V(t) - \frac{1}{2}\eta m(t)\Bigg] \\
&\quad - \frac{1}{\vartheta V(t) - \frac{1}{2}m(t)}\Bigg[-\vartheta\mu_0 V(t) \\
&\quad - \left(\vartheta\lambda_\alpha - \frac{1}{2}\kappa_1\right)\alpha(1,t)^2 - \left(\vartheta\lambda_\beta - \frac{1}{2}\kappa_2\right)\beta(0,t)^2 \\
&\quad - \frac{1}{2}\lambda_d d(t)^2 + \frac{1}{2}\eta m(t) + \frac{1}{2}\sigma V(t)\Bigg]\psi.
\end{aligned} \tag{81}$$

Applying $\kappa_1 \geq \max\{2\lambda_a, 2\vartheta\lambda_\alpha\}$, $\kappa_2 \geq \max\{2\lambda_a, 2\vartheta\lambda_\beta\}$, which are ensured by (47), (55), and applying the following inequalities $-\frac{\frac{1}{2}\eta m(t)}{\vartheta V(t) - \frac{1}{2}m(t)} \leq -\frac{\frac{1}{2}\eta m(t)}{-\frac{1}{2}m(t)} = \eta$, $\frac{V(t)}{\vartheta V(t) - \frac{1}{2}m(t)} \leq \frac{V(t)}{\vartheta V(t)} = \frac{1}{\vartheta}$, $\frac{d(t)^2}{\vartheta V(t) - \frac{1}{2}m(t)} = \frac{d(t)^2 + \frac{1}{2}m(t) - \frac{1}{2}m(t)}{\vartheta V(t) - \frac{1}{2}m(t)} \leq \psi(t) + 1$, which hold because of $m(t) < 0$, then (81) becomes

$$\dot{\psi}(t) \leq \frac{1}{2}\lambda_d\psi(t)^2 + (\lambda_a + 1 + \lambda_d + \eta + \mu_0)\psi(t) + 1 + \frac{1}{2}\lambda_d + \lambda_a + \frac{\lambda_a}{\xi_1\vartheta} + \eta. \tag{82}$$

The differential inequality (82) has the form $\dot{\psi} \leq n_1\psi^2 + n_2\psi + n_3$, where $n_1 = \frac{1}{2}\lambda_d$, $n_2 = \lambda_a + 1 + \lambda_d + \eta + \mu_0$, $n_3 = 1 + \frac{1}{2}\lambda_d + \lambda_a + \frac{\lambda_a}{\xi_1\vartheta} + \eta$, are positive constants. It follows that the time needed by ψ to go from 0 to 1 is at least

$$\underline{\tau} = \int_0^1 \frac{1}{n_3 + n_2 s + n_1\, s^2} ds > 0. \tag{83}$$

The proof of this claim is complete. ■

According to Claims 1 and 2, the proof of Lemma 3 is complete. ■

Next, we present the following lemmas regarding parameter convergence. In the rest of this article, when we say that $z[t]$, $w[t]$ are equal to zero for $x \in [0,1], t \in [\mu_{i+1}, t_{i+1}]$, or not identically zero on the same domain, we mean "except possibly for finitely many discontinuities of the functions $w[t], z[t]$." These discontinuities are isolated curves in the rectangle $[0,1] \times [\mu_{i+1}, t_{i+1}]$.

Lemma 4: The sufficient and necessary conditions of $Q_{n,1}(\mu_{i+1}, t_{i+1}) = 0$, $Q_{n,3}(\mu_{i+1}, t_{i+1}) = 0$ for $n = 1, 2, \ldots$ are $z[t] = 0$, $w[t] = 0$ on $t \in [\mu_{i+1}, t_{i+1}]$, respectively. The sufficient and necessary condition of $Q_4(\mu_{i+1}, t_{i+1}) = 0$ is $\zeta(t) = 0$ on $t \in [\mu_{i+1}, t_{i+1}]$.

Proof: The proof of that the sufficient and necessary conditions of $Q_{n,1}(\mu_{i+1}, t_{i+1}) = 0$, $Q_{n,3}(\mu_{i+1}, t_{i+1}) = 0$ for $n = 1, 2, \ldots$ are $z[t] = 0$, $w[t] = 0$ on $t \in [\mu_{i+1}, t_{i+1}]$, respectively, is the same as the proof of [40, Lem. 2], where the fact that $z \in C^0([t_i, t_{i+1}]; L^2(0,1))$, $w \in C^0([t_i, t_{i+1}]; L^2(0,1))$, and the set $\{\sqrt{2}\sin(n\pi x) : n = 1, 2, \ldots\}$ being an orthonormal basis of $L^2(0,1)$ have been used. By recalling (34), (36), it is straightforward to see that the sufficient and necessary condition of $Q_4(\mu_{i+1}, t_{i+1}) = 0$ is $\zeta(t) = 0$ on $t \in [\mu_{i+1}, t_{i+1}]$. The proof of Lemma 4 is complete. ■

Lemma 5: For the adaptive estimates defined by (63) based on the data in the interval $t \in [\mu_{i+1}, t_{i+1}]$, the following statements hold.

If $z[t]$ (or $w[t]$, or $\zeta(t)$) is not identically zero for $t \in [\mu_{i+1}, t_{i+1}]$, then $\hat{d}_3(t_{i+1}) = d_3$ (or $\hat{d}_2(t_{i+1}) = d_2$, or $\hat{a}(t_{i+1}) = a$, respectively).

If $z[t]$ (or $w[t]$, or $\zeta(t)$) is identically zero for $t \in [\mu_{i+1}, t_{i+1}]$, then $\hat{d}_3(t_{i+1}) = \hat{d}_3(t_i)$ (or $\hat{d}_2(t_{i+1}) = \hat{d}_2(t_i)$, or $\hat{a}(t_{i+1}) = \hat{a}(t_i)$, respectively).

Proof: We prove the following five results, from which the statements in this lemma are obtained.

1) *Result 1:* If $z[t]$ is not identically zero and $w[t]$ is identically zero on $t \in [\mu_{i+1}, t_{i+1}]$, then $\hat{d}_3(t_{i+1}) = d_3$, $\hat{d}_2(t_{i+1}) = \hat{d}_2(t_i)$; If $w[t]$ is not identically zero and $z[t]$ is identically zero on $t \in [\mu_{i+1}, t_{i+1}]$, then $\hat{d}_3(t_{i+1}) = \hat{d}_3(t_i)$, $\hat{d}_2(t_{i+1}) = d_2$. The proof of Result 1 is very similar to the proof of cases 1 and 2 in [40, Lem. 3], and thus, they are omitted.

2) *Result 2:* If $w[t]$, $z[t]$ are identically zero on $t \in [\mu_{i+1}, t_{i+1}]$, then $\hat{d}_3(t_{i+1}) = \hat{d}_3(t_i)$, $\hat{d}_2(t_{i+1}) = \hat{d}_2(t_i)$. The proof of Result 2 is shown as follows. In this case, $Q_{n,1}(\mu_{i+1}, t_{i+1}) = 0$, $Q_{n,2}(\mu_{i+1}, t_{i+1}) = 0$, $Q_{n,3}(\mu_{i+1}, t_{i+1}) = 0$, $H_{n,1}(\mu_{i+1}, t_{i+1}) = 0$, $H_{n,2}(\mu_{i+1}, t_{i+1}) = 0$ for $n = 1, 2, \ldots$ according to (30), (31), and (24)–(28). It follows that $S_i = \Theta$, and then (63) shows that $\hat{d}_3(t_{i+1}) = \hat{d}_3(t_i)$, $\hat{d}_2(t_{i+1}) = \hat{d}_2(t_i)$.

3) *Result 3:* If both $w[t]$ and $z[t]$ are not identically zero on $t \in [\mu_{i+1}, t_{i+1}]$, then $\hat{d}_3(t_{i+1}) = d_3$, $\hat{d}_2(t_{i+1}) = d_2$. The proof of Result 3 is shown as follows. According to Lemma 4, there exists $n \in \mathbb{N}$ such that $Q_{n,3}(\mu_{i+1}, t_{i+1}) \neq 0$ (or $Q_{n,1}(\mu_{i+1}, t_{i+1}) \neq 0$). Define the index set I_1 to be the set of all $n \in \mathbb{N}$ with $Q_{n,1}(\mu_{i+1}, t_{i+1}) \neq 0$ and define the index set I_2 to be the set of all $n \in \mathbb{N}$ with $Q_{n,3}(\mu_{i+1}, t_{i+1}) \neq 0$. Denote the elements in I_1 as $n_1 \in \mathbb{N}$ and those in I_2 as $n_2 \in \mathbb{N}$, i.e., $Q_{n_1,1}(\mu_{i+1}, t_{i+1}) \neq 0$, $Q_{n_2,3}(\mu_{i+1}, t_{i+1}) \neq 0$.

For the set S_i defined in (21), by virtue of (61)–(63), if S_i is a singleton then it is nothing else but the least-squares estimate

Authorized licensed use limited to: Xiamen University. Downloaded on March 16,2024 at 08:56:11 UTC from IEEE Xplore. Restrictions apply.

of the unknown vector of parameters (d_3, d_2) on the interval $[\mu_{i+1}, t_{i+1}]$, and $S_i = \{(d_3, d_2)\}$ according to (61), (62). From (21)–(23), we have

$$S_i \subseteq S_{ai} := \left\{(\ell_1, \ell_2) \in \Theta_1 : \ell_1 = \frac{H_{n_1,1}(\mu_{i+1}, t_{i+1})}{Q_{n_1,1}(\mu_{i+1}, t_{i+1})} - \ell_2 \frac{Q_{n_1,2}(\mu_{i+1}, t_{i+1})}{Q_{n_1,1}(\mu_{i+1}, t_{i+1})}, n_1 \in I_1\right\} \quad (84)$$

$$S_i \subseteq S_{bi} := \left\{(\ell_1, \ell_2) \in \Theta_1 : \ell_2 = \frac{H_{n_2,2}(\mu_{i+1}, t_{i+1})}{Q_{n_2,3}(\mu_{i+1}, t_{i+1})} - \ell_1 \frac{Q_{n_2,2}(\mu_{i+1}, t_{i+1})}{Q_{n_2,3}(\mu_{i+1}, t_{i+1})}, n_2 \in I_2\right\}. \quad (85)$$

We next prove by contradiction that $S_i = \{(d_3, d_2)\}$. Suppose that on the contrary $S_i \neq \{(d_3, d_2)\}$, i.e., S_i defined by (21) is not a singleton, which implies that the sets S_{ai}, S_{bi} defined by (84), (85) are not singletons (because either of S_{ai}, S_{bi} being a singleton implies that S_i is a singleton). It follows that there exist constants $\bar{\lambda} \in \mathbb{R}$, $\bar{\lambda}_1 \in \mathbb{R}$ such that

$$\frac{Q_{n_1,2}(\mu_{i+1}, t_{i+1})}{Q_{n_1,1}(\mu_{i+1}, t_{i+1})} = \bar{\lambda}_1, \ \frac{Q_{n_2,2}(\mu_{i+1}, t_{i+1})}{Q_{n_2,3}(\mu_{i+1}, t_{i+1})} = \bar{\lambda}, \quad (86)$$

where $n_1 \in I_1$ and $n_2 \in I_2$, because if there were two different indices $k_1, k_2 \in I_2$ with $\frac{Q_{k_1,2}(\mu_{i+1},t_{i+1})}{Q_{k_1,3}(\mu_{i+1},t_{i+1})} \neq \frac{Q_{k_2,2}(\mu_{i+1},t_{i+1})}{Q_{k_2,3}(\mu_{i+1},t_{i+1})}$, then the set S_{bi} defined by (85) would be a singleton, and the same would be the case with S_{ai} defined by (84) if there were two different indices $\bar{k}_1, \bar{k}_2 \in I_1$ with $\frac{Q_{\bar{k}_1,2}(\mu_{i+1},t_{i+1})}{Q_{\bar{k}_1,1}(\mu_{i+1},t_{i+1})} \neq \frac{Q_{\bar{k}_2,2}(\mu_{i+1},t_{i+1})}{Q_{\bar{k}_2,1}(\mu_{i+1},t_{i+1})}$. Moreover, since S_i is not a singleton, the definition (21) implies

$$Q_{n,2}(\mu_{i+1}, t_{i+1})^2 = Q_{n,1}(\mu_{i+1}, t_{i+1}) Q_{n,3}(\mu_{i+1}, t_{i+1}) \quad (87)$$

for all $n \in I_1 \cup I_2$ by recalling (23) (because if (87) does not hold, it follows from (23) that there exists $n \in I_1 \cup I_2$ such that $\det(\bar{G}_n(\mu_{i+1}, t_{i+1})) \neq 0$, which implies that S_i defined by (21) is a singleton: a contradiction). According to (26)–(28), (87), and the fact that the Cauchy–Schwarz inequality holds as an equality only when two functions are linearly dependent, we obtain the existence of the constants $\hat{\lambda}_{n_1} \in \mathbb{R}$, $\check{\lambda}_{n_2} \in \mathbb{R}$ such that

$$g_{n_1,2}(t, \mu_{i+1}) = \hat{\lambda}_{n_1} g_{n_1,1}(t, \mu_{i+1}), \quad n_1 \in I_1 \quad (88)$$

$$g_{n_2,1}(t, \mu_{i+1}) = \check{\lambda}_{n_2} g_{n_2,2}(t, \mu_{i+1}), \quad n_2 \in I_2 \quad (89)$$

for $t \in [\mu_{i+1}, t_{i+1}]$ (notice that $g_{n_1,1}(t, \mu_{i+1})$ and $g_{n_2,2}(t, \mu_{i+1})$ are not identically zero on $t \in [\mu_{i+1}, t_{i+1}]$ because of $Q_{n_1,1}(\mu_{i+1}, t_{i+1}) \neq 0$ and $Q_{n_2,3}(\mu_{i+1}, t_{i+1}) \neq 0$). Recalling (86), we obtain from (26)–(28) and (88), (89) that

$$g_{n_1,2}(t, \mu_{i+1}) = \bar{\lambda}_1 g_{n_1,1}(t, \mu_{i+1}), \quad n_1 \in I_1 \quad (90)$$

$$g_{n_2,1}(t, \mu_{i+1}) = \bar{\lambda} g_{n_2,2}(t, \mu_{i+1}), \quad n_2 \in I_2 \quad (91)$$

for $t \in [\mu_{i+1}, t_{i+1}]$. Equations (90), (91) holding is a necessary condition of the hypothesis that S_i is not a singleton.

Claim 3: If S_i is not a singleton, then $\bar{\lambda} \neq 0, \bar{\lambda}_1 \neq 0$ and $\bar{\lambda} = \frac{1}{\bar{\lambda}_1}$ in (90) and (91).

Proof: The proof is very similar to that of [40, Claim 1], and thus, it is omitted. ■

Claim 4: Equations (90), (91) ($\bar{\lambda} \neq 0, \bar{\lambda}_1 \neq 0$ and $\bar{\lambda} = \frac{1}{\bar{\lambda}_1}$) hold if and only if $z(x,t) - \bar{\lambda} w(x,t) = 0$ ($\bar{\lambda} \neq 0$) for $t \in [\mu_{i+1}, t_{i+1}]$, $x \in [0, 1]$.

Proof: With using Claim 3, the proof is very similar to that of [40, Claim 2], and thus it is omitted. ■

Claim 5: If $w(x,t)$ is not identically zero on $x \in [0, 1]$, $t \in [\mu_{i+1}, t_{i+1}]$, the function $z(x,t) - \bar{\lambda} w(x,t)$ ($\bar{\lambda} \neq 0$) is not identically zero on $x \in [0, 1]$, $t \in [\mu_{i+1}, t_{i+1}]$.

Proof: The proof is shown in Appendix C. ■

Recalling Claims 3, 4, and 5, we know that the equation set (90), (91), which is a necessary condition of the hypothesis that S_i is not a singleton, does not hold. Consequently, S_i is a singleton, i.e., $S_i = \{(d_3, d_2)\}$. Therefore, $\hat{d}_3(t_{i+1}) = d_3$, $\hat{d}_2(t_{i+1}) = d_2$.

4) *Result 4:* If $\zeta(t)$ is not identically zero for $t \in [\mu_{i+1}, t_{i+1}]$, then $\hat{a}(t_{i+1}) = a$. The proof of Result 4 is shown as follows. By virtue of (61)–(63), if $\bar{S}_i$ defined in (32) is a singleton, then $\hat{a}(t_{i+1}) = a$. According to Lemma 4, $Q_4(\mu_{i+1}, t_{i+1}) \neq 0$. It follows that $\bar{S}_i$ is a singleton. Therefore, we obtain $\hat{a}(t_{i+1}) = a$.

5) *Result 5:* If $\zeta(t)$ is identically zero for $t \in [\mu_{i+1}, t_{i+1}]$, then $\hat{a}(t_{i+1}) = \hat{a}(t_i)$. The proof of Result 5 is shown as follows. According to (33), (34), (36), we have that $Q_4(\mu_{i+1}, t_{i+1}) = 0$, $H_3(\mu_{i+1}, t_{i+1}) = 0$. We then obtain that the set $\bar{S}_i = \{|\ell_3| \leq \bar{a}\}$. Recalling (63), we have that $\hat{a}(t_{i+1}) = \hat{a}(t_i)$.

From the above five results, we obtain Lemma 5. ■

Lemma 6: If $\hat{d}_3(t_i) = d_3$ (or $\hat{d}_2(t_i) = d_2$, or $\hat{a}(t_i) = a$) for certain $i \in \mathbb{Z}^+$, then $\hat{d}_3(t) = d_3$ (or $\hat{d}_2(t) = d_2$, or $\hat{a}(t) = a$, respectively) for all $t \in [t_i, \lim_{k\to\infty}(t_k))$.

Proof: According to Lemma 5, we have that $\hat{d}_3(t_{i+1})$ is equal to either d_3 or $\hat{d}_3(t_i)$. Therefore, if $\hat{d}_3(t_i) = d_3$, then $\hat{d}_3(t) = d_3$ for all $t \in [t_i, \lim_{k\to\infty}(t_k))$. The same is true of $\hat{d}_2$ and $\hat{a}$. The proof is complete. ■

We are now ready to provide the proof of Theorem 1.

Proof: 1) We now prove the first of the three portions of the theorem. Recalling Lemma 3, we have that $t_i \geq \min\{\underline{r}, \underline{\tau}\}(i-1)$, $i \geq 1$, which yields $\lim_{i\to\infty}(t_i) = +\infty$. Then the well-posedness of the closed-loop system is obtained by recalling Proposition 1. The property 1) is, thus, obtained. The fact that $\lim_{i\to\infty}(t_i) = +\infty$ allows the solution to be defined on $\mathbb{R}_+$ in the following analysis.

2) We now prove the second of the three portions of the theorem. First, we propose the following claim about the sufficient and necessary condition of the finite-time convergence of parameter estimates to the true values.

Claim 6: When $\hat{d}_3(0) \neq d_3$ (or $\hat{d}_2(0) \neq d_2$, or $\hat{a}(0) \neq a$), the estimate $\hat{d}_3(t)$ (or $\hat{d}_2(t)$, or $\hat{a}(t)$) reaches the actual value d_3 (or d_2, or a) in finite time if and only if $z[t]$ (or $w[t]$, or $\zeta(t)$, respectively) is not identically zero on $t \in [0, \infty)$.

Proof: The proof is shown in the Appendix D. ■

Claim 7: If any one of the three estimates $\hat{d}_3(t), \hat{d}_2(t), \hat{a}(t)$ does not reach the true value in finite time, it implies that $\Omega(t) \equiv 0$ on $t \in [\frac{1}{q_1}, \infty)$ and that $m(t)$ is exponentially convergent to zero.

Proof: The proof is shown in the Appendix E. ■

Next, we estimate the maximum convergence time of the parameter estimates when they reach the true values.

Claim 8: If the parameter estimate $\hat{\theta}(t)$ reaches the true value θ in finite time, i.e., t_ε, then $t_\varepsilon \leq \frac{1}{q_1} + \frac{1}{q_2} + T$.

Proof: The proof is shown in the Appendix F.

According to Claims 7 and 8, the proof of the property 2) is complete.

3) We now prove the last of the three portions of the theorem. Define a Lyapunov function as

$$V_a(t) = V(t) - \mu m(t) \quad (92)$$

Authorized licensed use limited to: Xiamen University. Downloaded on March 16,2024 at 08:56:11 UTC from IEEE Xplore. Restrictions apply.

where $m(t)$ is defined in (46) ($m(t) < 0$ is shown in Lemma 2), the positive constant μ is defined in (52), and $V(t)$ is given in (44). Recalling (76), (77), applying the Cauchy–Schwarz inequality into the backstepping transformation (6), (7) and its inverse (8), (9), we have

$$\xi_3\bar{\Omega}(t) \le V_a(t) \le \xi_4\bar{\Omega}(t) \tag{93}$$

for some positive ξ_3, ξ_4, where the definition of $\bar{\Omega}(t)$ is given in (66). Taking the derivative of (92) along (10)–(13), recalling the equalities (46), (78), inserting (71), and applying Young's inequality and the Cauchy–Schwarz inequality, we have

$$\begin{aligned}\dot{V}_a(t) \le& -\frac{1}{2}a_{\mathrm{m}}\zeta(t)^2 - \left(\frac{1}{2}q_1e^{-\delta_2} - \mu\kappa_1\right)\alpha(1,t)^2\\ &- \left(\frac{1}{2}q_2r_a - \frac{b^2}{2a_{\mathrm{m}}} - \frac{p^2}{2}q_1 - \mu\kappa_2\right)\beta(0,t)^2\\ &+ \left(q_2r_ae^{\delta_1}c_0^2 - \mu\lambda_d\right)d(t)^2 + q_2r_ae^{\delta_1}c_0^2\xi(t)^2\\ &- \left(\frac{1}{2}\delta_1q_2r_a - r_a|d_4|\right)\int_0^1 e^{\delta_1x}\beta(x,t)^2dx + \mu\eta m(t)\\ &- \left(\frac{1}{2}\delta_2q_1 - |d_1|\right)\int_0^1 e^{-\delta_2x}\alpha(x,t)^2dx + \mu\sigma V(t)\end{aligned} \tag{94}$$

for $t \ge 0$. Because of (64), according to (20), we have

$$\xi(t) \equiv 0, \quad t \in [t_\varepsilon, \infty). \tag{95}$$

Recalling the conditions of δ_1, δ_2, r_a, λ_d, μ in (45), (50), and (52), we arrive at

$$\begin{aligned}\dot{V}_a(t) \le& -(\nu_a - \mu\sigma)V + \mu\eta m(t)\\ =& -(\nu_a - \mu\sigma)V_a + (-\mu(\nu_a - \mu\sigma) + \mu\eta)\,m(t)\end{aligned} \tag{96}$$

for $t \ge t_\varepsilon$, where (76), (77), (92), (95) and the fact that $a_{\mathrm{m}} \ge b\kappa - \bar{a} > 0$ have been used, and where the positive constant ν_a is given in (53). Recalling σ, η in (51), we arrive at

$$\dot{V}_a(t) \le -\lambda_1V_a(t), \quad t \ge t_\varepsilon \tag{97}$$

where $\lambda_1 = \nu_a - \mu\sigma > 0$. Multiplying both sides of (97) by $e^{\lambda_1 t}$ and integrating both sides of (97) from t_ε to t, we obtain $V_a(t) \le V_a(t_\varepsilon)e^{-\lambda_1(t-t_\varepsilon)}$, $t \ge t_\varepsilon$. Recalling (93), we have

$$\bar{\Omega}(t) \le \Upsilon_\theta\bar{\Omega}(t_\varepsilon)e^{-\lambda_1(t-t_\varepsilon)}, \quad t \ge t_\varepsilon \tag{98}$$

where the positive constant Υ_θ is

$$\Upsilon_\theta = \frac{\xi_4}{\xi_3}. \tag{99}$$

If $t_\varepsilon = 0$, the property 3), i.e., (65), is obtained directly. Next, we conduct analysis for $t \in [0, t_\varepsilon]$ with $t_\varepsilon \ne 0$. Recalling (45), (50), (51), (52), (76), (77), (92), (94), we obtain

$$\dot{V}_a(t) \le -\lambda_1V_a(t) + Q(\hat{\theta}(0))V_a(t), \quad t \in [0, t_\varepsilon] \tag{100}$$

where the positive constant $Q(\hat{\theta}(0))$ is obtained by bounding $\xi(t)^2$ given by (70), and the value of $Q(\hat{\theta}(0))$ depends on the initial estimate $\hat{\theta}(0)$. We, thus, obtain

$$\bar{\Omega}(t) \le \Upsilon_\theta\bar{\Omega}(0)e^{\lambda_2(\hat{\theta}(0))t}, \quad t \in [0, t_\varepsilon] \tag{101}$$

where $\lambda_2(\hat{\theta}(0)) = |Q(\hat{\theta}(0)) - \lambda_1| > 0$, and the positive constant Υ_θ is given in (99). Therefore, we have

$$\bar{\Omega}(t_\varepsilon) \le \Upsilon_\theta e^{\lambda_2(\hat{\theta}(0))t_\varepsilon}\bar{\Omega}(0). \tag{102}$$

Inserting (102) into (98) and applying Claim 8, yields

$$\bar{\Omega}(t) \le \Upsilon_\theta^2 e^{(\lambda_2(\hat{\theta}(0))+\lambda_1)(\frac{1}{q_1}+\frac{1}{q_2}+T)}\bar{\Omega}(0)e^{-\lambda_1 t}, \quad t \ge 0. \tag{103}$$

Denoting $M = \Upsilon_\theta^2 e^{(\lambda_2(\hat{\theta}(0))+\lambda_1)(\frac{1}{q_1}+\frac{1}{q_2}+T)}$, we obtain (65). This completes the proof of the property 3) of the theorem. ■

TABLE I
PHYSICAL PARAMETERS OF THE MINING CABLE ELEVATOR

Parameters (units)	values
Cable length L (m)	2000
Cable diameter R_d (m)	0.2
Cable effective Young's Modulus E (N/m^2)	1.02×10^9
Cable linear density ρ (kg/m)	8.1
Mass of cage M_c (kg)	15000
Damping coefficient of cage c_L	0.4
Cable material damping coefficient d_c	0.5
Gravitational acceleration g (m/s^2)	9.8

VI. Application to Mining Cable Elevator

A. Model

The axial vibration model of the mining cable elevator is described by the following wave PDE-ODE model with in-domain damping [43]:

$$\rho u_{tt}(x,t) = \frac{\pi R_d^2}{4}Eu_{xx}(x,t) - d_cu_t(x,t) \tag{104}$$

$$M_cu_{tt}(0,t) = -c_Lu_t(0,t) + \frac{\pi R_d^2}{4}Eu_x(0,t) \tag{105}$$

$$\frac{\pi R_d^2}{4}Eu_x(L,t) = U_d(t) \tag{106}$$

where the cable length is considered as constant. The PDE state $u(x,t)$ denotes the distributed axial vibration displacements along the cable, and the boundary state $u(0,t)$ represents the axial vibration displacement of the cage. The physical parameters in (104)–(106) are shown in Table I.

According to [28], we apply the Riemann transformations $z(x,t) = u_t(x,t) - \sqrt{\frac{E\pi}{\rho}}\frac{R_d}{2}u_x(x,t)$, $w(x,t) = u_t(x,t) + \sqrt{\frac{E\pi}{\rho}}\frac{R_d}{2}u_x(x,t)$, and define the new variable $\zeta(t) = u_t(0,t)$, which allows us to rewrite (104)–(106) as (1)–(5) with the coefficients

$$q_1 = q_2 = \sqrt{\frac{E\pi}{\rho}}\frac{R_d}{2}, \quad d_1 = d_2 = d_3 = d_4 = \frac{-d_c}{2\rho} \tag{107}$$

$$p = 1, \quad c = 2, \quad c_0 = \frac{4}{R_d\sqrt{E\pi\rho}} \tag{108}$$

$$a = \frac{-c_L}{M_c} - \frac{R_d\sqrt{E\pi\rho}}{2M_c}, b = \frac{R_d\sqrt{E\pi\rho}}{2M_c} \tag{109}$$

where a reflection term $z(L,t)$ appearing at the controlled boundary (5) is considered to be compensated by the control input at the drum [37] independent of the head sheave control input designed in this article. The unknown physical parameters are damping coefficients of the cable and the cage, d_c, c_L, which leads to the fact that a is unknown and $d_1 = d_2 = d_3 = d_4$ are unknown in the 2×2 hyperbolic PDE-ODE system. The designs in this article are directly applicable to this problem (with only one slight modification: removing the last term in (29) and multiplying (30), (31) by 2), and the outputs of the identifer are the estimates of d_2, d_3. According to the values in Table I, together with (107)–(109), we know that Assumptions 1 and 2 are

Authorized licensed use limited to: Xiamen University. Downloaded on March 16,2024 at 08:56:11 UTC from IEEE Xplore. Restrictions apply.

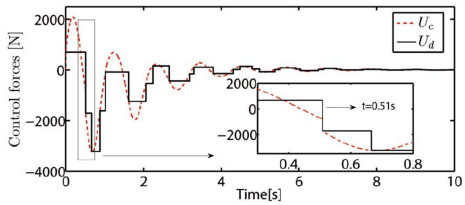

Fig. 2. Continuous-in-state control signal $U_c(t)$ in (18) and the piecewise-constant control signal $U_d(t)$ in (17).

satisfied. The bounds $\bar{a}, \bar{d}_3, \bar{d}_2$ of the unknown parameters $a = 1.07, d_3 = d_2 = -0.025$ are set as, $3, 0.4, 0.5$, respectively. The initial conditions of $z(x,t)$ and $w(x,t)$ are defined as $z(x,0) = 0.5\sin(2\pi x/L + \pi/6)$, $w(x,0) = 0.5\sin(3\pi x/L)$ and $\zeta(0) = \frac{1}{2}(pw(0,0) + z(0,0))$ according to (4). We pick the initial value of $m(t)$ as $m(0) = -10$.

B. Determination of Design Parameters

The free design parameters δ, T in (40) are selected as $\delta = 1.8$, $T = 3$, and the positive integer n in the parameter estimator (63) is defined as 7. According to (107)–(109), the parameter values in Table I, and the known bounds $\bar{a}, \bar{d}_3, \bar{d}_2$ defined earlier, recalling (15), (45), the design parameters $\kappa, \delta_1, \delta_2, r_a$ are determined to be $\kappa = -10$, $\delta_1 = 0.1$, $\delta_2 = 0.1$, $r_a = 1.5$. Choose the design parameter $\underline{r}$ as $\underline{r} = 0.2$ via (42). Next, choose $\kappa_1 = 2100, \kappa_2 = 3000$ according to (47), where $\lambda_\alpha = 899.6$, $\lambda_\beta = 1490.8$ are obtained from (48), and a conservative estimate $\lambda_a = 1000$ comes from (49). Then, the design parameters λ_d, σ, η are selected as $\lambda_d = 0.005, \sigma = 60, \eta = 120$ to satisfy (50), (51), where $\mu = 0.15, \nu_a = 9.66$ are obtained from (52), (53). Finally, pick the design parameter $\vartheta = 12000$ via (55). Some notes on tuning the design parameters are given as follows. The appropriate increase of $\kappa_1, \kappa_1, \delta_1, r_a$ can reduce the triggering times, however, accompanied by decrease of the convergence rate of the plant norms. Even though the appropriate increase of η, λ_d, δ_2 and decrease of ϑ will generate more triggering times in the evolution, it will improve the convergence rate of the plant norms. The increase of the gain κ will fasten the convergence to zero of the plant norms, however, which will also lead to more frequent updates.

C. Simulation Results

We stimulate a mining cable elevator running in a short time period of 10 s, where the cable length is regarded as constant. The simulation is conducted based on the finite difference method with a time step of 0.0015 s and a space step of 0.5 m. By employing the finite-difference method as well, with a step length of 0.5 m for y running from 0 to x, the approximate solutions of $\Psi(x,y;\hat{\theta}(t_i))$, $\Phi(x,y;\hat{\theta}(t_i))$, $\lambda(x;\hat{\theta}(t_i))$ in the control law (17) are obtained from the conditions (A.7)–(A.12), whose unknown coefficients are replaced by the piecewise-constant estimates. The triggering mechanism (37)–(41) is implemented as the flowchart in Fig. 1, with the design parameters selected in Section VI-B.

The piecewise-constant control input $U_d(t)$ defined in (17) is shown in Fig. 2, where the estimate $\hat{\theta}$ is recomputed and the states z, w, ζ are resampled simultaneously. The first update is triggered at $t = 0.51$ s, the total number of triggering times is 33, the maximum dwell time is 0.595 s, and the minimal dwell time

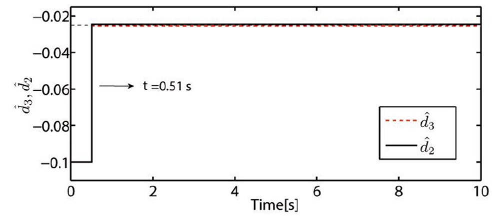

Fig. 3. Parameter estimates $\hat{d}_3$ and $\hat{d}_2$.

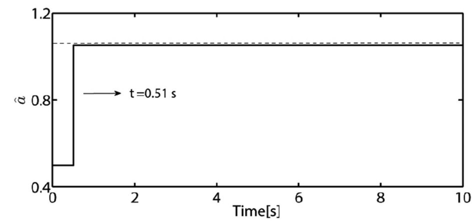

Fig. 4. Parameter estimate $\hat{a}$.

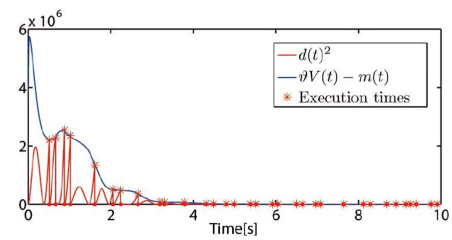

Fig. 5. Evolution of $d(t)^2$ and $\vartheta V(t) - m(t)$ in (38).

is 0.105 s, which is much larger than the highly conservative minimal dwell-time estimate of 5.75×10^{-4} s obtained from Lemma 3 and (83), where the analysis parameter μ_0 defined in (80) is $\mu_0 = 331$. The continuous-in-state control signal $U_c(t)$ (18) used in ETM is also shown in Fig. 2. There is a jump in the continuous-in-state signal $U_c(t)$ at $t = 0.51$ s, because $U_c(t)$ defined in (18) includes the piecewise-constant parameter estimate $\hat{\theta}$ whose evolution is shown in Figs. 3 and 4, where, under the nonzero initial conditions defined at the beginning of this section, the estimates $\hat{d}_3, \hat{d}_2, \hat{a}$ are updated and reach the true values of the unknown parameters $d_3 = -0.025, d_2 = -0.025, a = 1.06$ (black dash lines) at the first triggering time, $t = 0.51$ s, and are kept constant in the subsequent re-computations. As shown in Figs. 2–4, both components (the control input and parameter estimate) in the proposed adaptive control are piecewise-constant. By contrast, in the existing adaptive methods, at most one component in the adaptive control (either the control input or the parameter estimate) employs piecewise-constant values, such as [2], [3], [40]–[42]. This makes the proposed adaptive method more suitable in control of mining cable elevators or other industry plants with large actuator's inertia, because the frequent movement of the massive actuator can be avoided.

Because the estimates have reached the true values at the first triggering time, according to the designed triggering mechanism (37)–(41), the following execution times are determined by the triggering condition (38), which can be seen in Fig. 5 showing the time evolution of the functions in the triggering condition (38) and the execution times. Fig. 5 shows that an event is generated, the control value is updated and $d(t)$ is reset to zero,

Authorized licensed use limited to: Xiamen University. Downloaded on March 16,2024 at 08:56:11 UTC from IEEE Xplore. Restrictions apply.

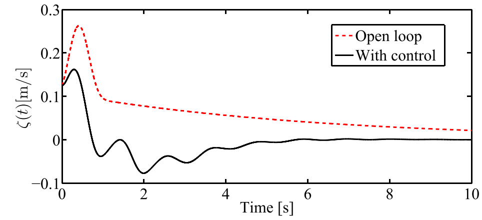

Fig. 6. Evolution of $\zeta(t)$ in open loop and under the control input $U_d(t)$ in (17).

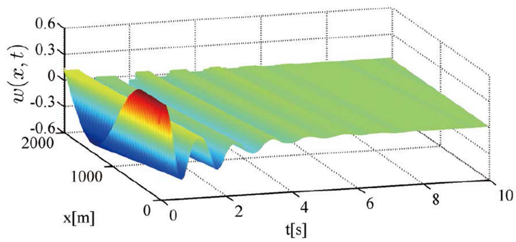

Fig. 7. Evolution of $w(x,t)$ under the control input $U_d(t)$ in (17).

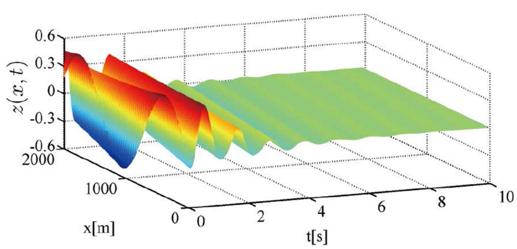

Fig. 8. Evolution of $z(x,t)$ under the control input $U_d(t)$ in (17).

when the trajectory $d(t)^2$ reaches the trajectory $\vartheta V(t) - m(t)$. Fig. 6 demonstrates that the state $\zeta(t)$ of the ODE connected at the uncontrolled boundary, whose physical meaning is the axial vibration velocity of the cage, is convergent and reaches zero at around 6 s under the proposed boundary control input, i.e., the control forces at the head sheave, while it will take more than 10 s in open loop. That is, the proposed controller improves the convergence rate in the open-loop dynamics. Figs. 7 and 8 show that the PDE states $z(x,t), w(x,t)$ are regulated to zero under the control input $U_d(t)$ as well, whose convergence rate is also larger than the ones in open loop (the results of $z(x,t)$, $w(x,t)$ in open loop are omitted here due to the space limit). Therefore, according to the Riemann transformation presented in Section VI-A, we find that the vibration energy of the cable $\frac{1}{2}\rho\|u_t(\cdot,t)\|^2 + \frac{R_d^2\pi}{8}E\|u_x(\cdot,t)\|^2$ also decreases to zero. Finally, we run simulations for 8 different initial conditions and compute the inter-execution times between two triggering times. The density of the inter-execution times is shown in Fig. 9, from which we know that the prominent inter-execution times are in the range from 0.1 s to 0.2 s.

VII. Conclusion

In this article, we have proposed an adaptive boundary control scheme, where both of the parameter estimates and control input employ piecewise-constant values, for a 2×2 hyperbolic PDE-ODE system, where two coefficients of the in-domain couplings between two transport PDEs, and the system parameter of a

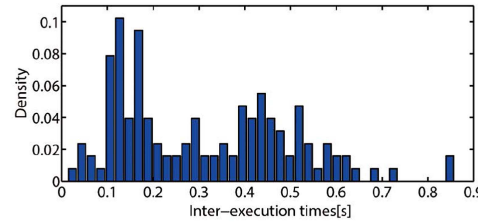

Fig. 9. Density of the inter-execution times computed for eight different initial conditions given by $z(x,0) = 0.5\sin(2\bar{n}\pi x/L + \pi/6) + \bar{k}(x/L)^2$, $w(x,0) = 0.5\sin(3\bar{m}\pi x/L) + \bar{k}(x/L)^2$ for $\bar{n} = 1,2$, $\bar{m} = 1,2$, $\bar{k} = 0,1$.

scalar ODE are unknown. The controller consists of a nominal continuous-in-time control signal, a batch least-squares identifier, and a triggering mechanism to determine the synchronous update times of both the parameter identifier and plant states in the control law. We have proved that the proposed control guarantees the following:

1) no Zeno phenomenon occurs;
2) parameter estimates are convergent to the true values in finite time in most situations;
3) the plant states are exponentially regulated to zero.

The effectiveness of the proposed design is verified by numerical simulation in the application of axial vibration control of a mining cable elevator with unknown cable and cage damping coefficients.

The proposed adaptive scheme is limited to dealing with the constant unknown parameters. In the future, an extension, where the unknown parameters vary in the piecewise-constant fashion, will be conducted. Also, the time delay, which often exists in the reality of applications, will be considered as well.

Appendix

A. Conditions of Kernels in the Backstepping Transformation (6), (7) and Its Inverse (8), (9)

The conditions of kernels $\varphi, \phi, \gamma, \Psi, \Phi, \lambda$ in the backstepping transformation (6), (7) are

$$d_2 - (q_1 + q_2)\varphi(x,x) = 0 \tag{A.1}$$

$$-\gamma(x)b + q_2\varphi(x,0) + q_1 p\phi(x,0) = 0 \tag{A.2}$$

$$-q_1\phi_x(x,y) - q_1\phi_y(x,y) - d_3\varphi(x,y) = 0 \tag{A.3}$$

$$q_2\varphi_y(x,y) - q_1\varphi_x(x,y) - (d_4 - d_1)\varphi(x,y) - d_2\phi(x,y) = 0 \tag{A.4}$$

$$q_1\gamma'(x) + (a - d_1)\gamma(x) + q_1 c\phi(x,0) = 0 \tag{A.5}$$

$$\gamma(0) = -p\kappa + c \tag{A.6}$$

$$d_3 + (q_1 + q_2)\Psi(x,x) = 0 \tag{A.7}$$

$$-\lambda(x)b + q_2\Phi(x,0) + q_1 p\Psi(x,0) = 0 \tag{A.8}$$

$$-q_1\Psi_y(x,y) + q_2\Psi_x(x,y) + (d_4 - d_1)\Psi(x,y) - d_3\Phi(x,y) = 0 \tag{A.9}$$

$$q_2\Phi_y(x,y) + q_2\Phi_x(x,y) - d_2\Psi(x,y) = 0 \tag{A.10}$$

$$-q_2\lambda'(x) + (a - d_4)\lambda(x) + q_1 c\Psi(x,0) = 0 \tag{A.11}$$

Authorized licensed use limited to: Xiamen University. Downloaded on March 16,2024 at 08:56:11 UTC from IEEE Xplore. Restrictions apply.

$$\lambda(0) = -\kappa. \tag{A.12}$$

The conditions of kernels $\bar{\varphi}, \bar{\phi}, \bar{\gamma}, \bar{\Psi}, \bar{\Phi}, \bar{\lambda}$ in the inverse backstepping transformation (8), (9) are

$$-d_3 + (q_1+q_2)\bar{\Psi}(x,x) = 0 \tag{A.13}$$

$$\bar{\lambda}(x)b - q_2\bar{\Phi}(x,0) - q_1 p\bar{\Psi}(x,0) = 0 \tag{A.14}$$

$$-q_1\bar{\Psi}_y(x,y) + q_2\bar{\Psi}_x(x,y) + (d_4-d_1)\bar{\Psi}(x,y) + d_3\bar{\phi}(x,y) = 0 \tag{A.15}$$

$$q_2\bar{\Phi}_y(x,y) + q_2\bar{\Phi}_x(x,y) + d_3\bar{\varphi}(x,y) = 0 \tag{A.16}$$

$$-q_2\bar{\lambda}'(x) - (b\kappa - a + d_4)\bar{\lambda}(x) - d_3\bar{\gamma}(x) = 0 \tag{A.17}$$

$$\bar{\lambda}(0) = \kappa \tag{A.18}$$

$$-d_2 - (q_1+q_2)\bar{\varphi}(x,x) = 0 \tag{A.19}$$

$$\bar{\gamma}(x)b - q_2\bar{\varphi}(x,0) - q_1 p\bar{\phi}(x,0) = 0 \tag{A.20}$$

$$q_2\bar{\varphi}_y(x,y) - q_1\bar{\varphi}_x(x,y) - (d_4-d_1)\bar{\varphi}(x,y) + d_2\bar{\Phi}(x,y) = 0 \tag{A.21}$$

$$-q_1\bar{\phi}_x(x,y) - q_1\bar{\phi}_y(x,y) + d_2\bar{\Psi}(x,y) = 0 \tag{A.22}$$

$$q_1\bar{\gamma}'(x) - (b\kappa - a + d_1)\bar{\gamma}(x) - d_2\bar{\lambda}(x) = 0 \tag{A.23}$$

$$\bar{\gamma}(0) = -p\kappa - c. \tag{A.24}$$

The equation sets (A.1)–(A.12) and (A.13)–(A.24) are well-known coupled linear heterodirectional hyperbolic PDE-ODE systems, whose well-posedness has been proved in [11, Th. 4.1].

B. Expressions of the Functions $M_1,\ldots,M_6$, K_1, K_2, K_3, and $\tilde{K}_1, \tilde{K}_2, \tilde{K}_3$

The expressions of the functions $M_1,\ldots,M_6$ are

$$M_1(y,\hat{\theta}(t_i),\theta) = q_1K_{1y}(y,\hat{\theta}(t_i),\theta) + K_1(y,\hat{\theta}(t_i),\theta)d_1 - q_2K_2(1,\hat{\theta}(t_i),\theta)\tilde{K}_1(y,\hat{\theta}(t_i),\theta) \tag{B.1}$$

$$M_2(y,\hat{\theta}(t_i),\theta) = q_2K_{2y}(y,\hat{\theta}(t_i),\theta) - K_2(y,\hat{\theta}(t_i),\theta)d_4 + q_2K_2(1,\hat{\theta}(t_i),\theta)\tilde{K}_2(y,\hat{\theta}(t_i),\theta) \tag{B.2}$$

$$M_3(\hat{\theta}(t_i),\theta) = K_3(\hat{\theta}(t_i),\theta)a_{\mathrm{m}} + q_2K_2(1,\hat{\theta}(t_i),\theta)\tilde{K}_3(\hat{\theta}(t_i),\theta) \tag{B.3}$$

$$M_4(\hat{\theta}(t_i),\theta) = K_3(\hat{\theta}(t_i),\theta)b - q_2K_2(0,\hat{\theta}(t_i),\theta) - pq_1K_1(0,\hat{\theta}(t_i),\theta) \tag{B.4}$$

$$M_5(\hat{\theta}(t_i),\theta) = q_1K_1(1,\hat{\theta}(t_i),\theta) \tag{B.5}$$

$$M_6(\hat{\theta}(t_i),\theta) = q_2c_0K_2(1,\hat{\theta}(t_i),\theta) \tag{B.6}$$

where the expressions of the functions K_1, K_2, K_3 are

$$K_1(y,\hat{\theta}(t_i),\theta) = \psi(1,y;\hat{\theta}(t_i)) - \int_y^1 \psi(1,\varepsilon;\hat{\theta}(t_i))\bar{\phi}(\varepsilon,y;\theta)d\varepsilon - \int_y^1 \Phi(1,\varepsilon;\hat{\theta}(t_i))\bar{\psi}(\varepsilon,y;\theta)d\varepsilon \tag{B.7}$$

$$K_2(y,\hat{\theta}(t_i),\theta) = \Phi(1,y;\hat{\theta}(t_i)) - \int_y^1 \psi(1,\varepsilon;\hat{\theta}(t_i))\bar{\varphi}(\varepsilon,y;\theta)d\varepsilon - \int_y^1 \Phi(1,\varepsilon;\hat{\theta}(t_i))\bar{\Phi}(\varepsilon,y;\theta)d\varepsilon \tag{B.8}$$

$$K_3(\hat{\theta}(t_i),\theta) = \lambda(1;\hat{\theta}(t_i)) - \int_0^1 \psi(1,y;\hat{\theta}(t_i))\bar{\gamma}(y;\theta)dy - \int_0^1 \Phi(1,y;\hat{\theta}(t_i))\bar{\lambda}(y;\theta)dy \tag{B.9}$$

and where the expressions of the functions $\tilde{K}_1, \tilde{K}_2, \tilde{K}_3$ are

$$\tilde{K}_1(y,\hat{\theta}(t_i),\theta) = \psi(1,y;\theta) - \psi(1,y;\hat{\theta}(t_i)) - \int_y^1 [\psi(1,\varepsilon;\theta) - \psi(1,\varepsilon;\hat{\theta}(t_i))]\bar{\phi}(\varepsilon,y;\theta)d\varepsilon - \int_y^1 [\Phi(1,\varepsilon;\theta) - \Phi(1,\varepsilon;\hat{\theta}(t_i))]\bar{\psi}(\varepsilon,y;\theta)d\varepsilon \tag{B.10}$$

$$\tilde{K}_2(y,\hat{\theta}(t_i),\theta) = \Phi(1,y;\theta) - \Phi(1,y;\hat{\theta}(t_i)) - \int_y^1 [\psi(1,\varepsilon;\theta) - \psi(1,\varepsilon;\hat{\theta}(t_i))]\bar{\varphi}(\varepsilon,y;\theta)d\varepsilon - \int_y^1 [\Phi(1,\varepsilon;\theta) - \Phi(1,\varepsilon;\hat{\theta}(t_i))]\bar{\Phi}(\varepsilon,y;\theta)d\varepsilon \tag{B.11}$$

$$\tilde{K}_3(\hat{\theta}(t_i),\theta) = \lambda(1;\theta) - \lambda(1;\hat{\theta}(t_i)) - \int_0^1 [\psi(1,y;\theta) - \psi(1,y;\hat{\theta}(t_i))]\bar{\gamma}(y;\theta)dy - \int_0^1 [\Phi(1,y;\theta) - \Phi(1,y;\hat{\theta}(t_i))]\bar{\lambda}(y;\theta)dy. \tag{B.12}$$

C. Proof of Claim 5

We prove this by contradiction. Suppose that there exists a $\bar{\lambda} \neq 0$ such that

$$z(x,t) - \bar{\lambda}w(x,t) \equiv 0, \quad x\in[0,1],\ t\in[\mu_{i+1}, t_{i+1}). \tag{C.1}$$

Taking the time and spatial derivatives of (C.1) yields

$$z_t(x,t) - \bar{\lambda}w_t(x,t) = 0,\ z_x(x,t) - \bar{\lambda}w_x(x,t) = 0 \tag{C.2}$$

for $x\in[0,1]$, $t\in[\mu_{i+1}, t_{i+1})$ (except possibly for finitely many discontinuities of the functions $w[t], z[t]$). Recalling (2), (3), we have

$$w_x(x,t) = \frac{d_3\bar{\lambda}^2 + (d_4-d_1)\bar{\lambda} - d_2}{-\bar{\lambda}(q_1+q_2)}w(x,t) \tag{C.3}$$

$$z_x(x,t) = \frac{d_3\bar{\lambda}^2 + (d_4-d_1)\bar{\lambda} - d_2}{-\bar{\lambda}(q_1+q_2)}z(x,t) \tag{C.4}$$

Authorized licensed use limited to: Xiamen University. Downloaded on March 16,2024 at 08:56:11 UTC from IEEE Xplore. Restrictions apply.

for $x\in[0,1], t\in[\mu_{i+1},t_{i+1})$. The solutions of (C.3), (C.4) are obtained as

$$w(x,t)=w(0,t)e^{\frac{d_3\bar\lambda^2+(d_4-d_1)\bar\lambda-d_2}{-\bar\lambda(q_1+q_2)}x} \tag{C.5}$$

$$z(x,t)=\bar\lambda w(0,t)e^{\frac{d_3\bar\lambda^2+(d_4-d_1)\bar\lambda-d_2}{-\bar\lambda(q_1+q_2)}x} \tag{C.6}$$

for $x\in[0,1], t\in[\mu_{i+1},t_{i+1})$, where $z(0,t)=\bar\lambda w(0,t)$, obtained from the hypothesis (C.1), has been used.

By virtue of (5), (17), we know that $w(1,t)$ is constant on $t\in[\mu_{i+1},t_{i+1})$. It implies that $w(0,t)$ is constant on $t\in[\mu_{i+1},t_{i+1})$ recalling (C.5), i.e.,

$$w(0,t)=w(0,\mu_{i+1}),\quad t\in[\mu_{i+1},t_{i+1}) \tag{C.7}$$

where $w(0,\mu_{i+1})\neq 0$, which is obtained from the fact that $w(x,t)$ is not identically zero in the interval and (C.5), (C.7). According to the hypothesis (C.1), we also have

$$z(0,t)=\bar\lambda w(0,\mu_{i+1}),\quad t\in[\mu_{i+1},t_{i+1}). \tag{C.8}$$

By virtue of (3), (C.1), (C.3)–(C.8), we obtain

$$q_2\frac{d_3\bar\lambda^2+(d_4-d_1)\bar\lambda-d_2}{-\bar\lambda(q_1+q_2)}+d_3\bar\lambda+d_4=0 \tag{C.9}$$

which is a necessary condition for the hypothesis (C.1) to hold.

For the case that $c\neq 0$, $a\neq 0$, inserting (C.7), (C.8) into (4), yields that $\zeta(t)=\frac{(\bar\lambda+p)}{c}w(0,\mu_{i+1})$ is also constant on $t\in[\mu_{i+1},t_{i+1})$. Recalling (1), and $w(0,\mu_{i+1})\neq 0$, it follows that

$$\bar\lambda=-\frac{bc}{a}-p. \tag{C.10}$$

For the cases that $c=0$, we have

$$\bar\lambda=-p \tag{C.11}$$

according to (4), (C.7), (C.8), and $w(0,\mu_{i+1})\neq 0$.

By virtue of Assumption 2, (C.10), and (C.11), we know that the necessary condition for the hypothesis (C.1) to hold, i.e., (C.9), does not hold for the cases that $a\neq 0$ and the case that $a=0, c=0$. For the case that $a=0$, $c\neq 0$, inserting (C.7), (C.8) into (4), recalling (1), and $w(0,\mu_{i+1})\neq 0$, it follows that $\bar\lambda=0$: contradiction. Therefore, the hypothesis (C.1) does not hold. The proof of this claim is complete.

D. Proof of Claim 6

We first prove sufficiency. If $z[t]$ (or $w[t]$, or $\zeta(t)$) is not identically zero for $t\in[0,\infty)$, there exists an interval $[\mu_{i+1},t_{i+1}]$ on which $z[t]$ (or $w[t]$, or $\zeta(t)$, respectively) is not identically zero. It follows that $\hat d_3(t_{i+1})=d_3$ (or $\hat d_2(t_{i+1})=d_2$, or $\hat a(\tau_{i+1})=a$, respectively), recalling Lemma 5.

Next, we prove necessity. When $\hat d_3(0)\neq d_3$ (or $\hat d_2(0)\neq d_2$, or $\hat a(0)\neq a$), if $z[t]$ (or $w[t]$, or $\zeta(t)$) is identically zero for $t\in[0,\infty)$, applying Lemma 5, we have $\hat d_3(t)=\hat d_3(0)\neq d_3$ (or $\hat d_2(t)=\hat d_2(0)\neq d_2$, or $\hat a(t)=\hat a(0)\neq a$, respectively). Therefore, if the estimate $\hat d_3$ (or $\hat d_2$, or $\hat a$) reaches the true value, it follows that $z[t]$ (or $w[t]$, or $\zeta(t)$, respectively) is not identically zero on $t\in[0,\infty)$.

The proof of Claim 6 is complete.

E. Proof of Claim 7

The proof is divided into the following three cases.

Case 1: We suppose that the estimate $\hat d_2(t)$ does not reach d_2 in finite time. It implies that $w[t]\equiv 0$ on $t\in[0,\infty)$ according to Claim 6. By virtue of (3) and $d_3\neq 0$, we have that $z[t]\equiv 0$ on $t\in[0,\infty)$. We then obtain from (4) that $\zeta(t)\equiv 0$ on $t\in[0,\infty)$. Therefore, $\Omega(t)\equiv 0$. According to $w[t]\equiv 0$, $z[t]\equiv 0$, and $\zeta(t)\equiv 0$ on $t\in[0,\infty)$, we have that $d(t)\equiv 0$ according to (19), and $m(t)$ is exponentially convergent to zero recalling (46) and (6), (7), (44).

Case 2: We suppose that the estimate $\hat d_3(t)$ does not reach d_3 in finite time. It implies that $z[t]\equiv 0$ on $t\in[0,\infty)$ according to Claim 6. Then, (1)–(5) become

$$\zeta(t)=e^{(a+b\frac{c}{p})t}\zeta(0) \tag{E.1}$$

$$w_t(x,t)=q_2w_x(x,t)+d_4w(x,t) \tag{E.2}$$

$$w(0,t)=\frac{c}{p}\zeta(t) \tag{E.3}$$

$$w(1,t)=c_0U_d(t) \tag{E.4}$$

$t\in[0,\infty)$, in the closed-loop system.

If $\zeta(0)=0$, then $z[t],w[t],\zeta(t)$ are identically zero on $t\in[0,\infty)$ according to (E.1)–(E.3), i.e., $\Omega(t)\equiv 0$.

Next we discuss the case when $\zeta(0)\neq 0$. Equation (E.3) holding for $t\in[0,\infty)$ requires the initial condition of w to be

$$w(x,0)=e^{-\frac{d_4}{q_2}x}\frac{c}{p}e^{(a+b\frac{c}{p})\frac{1}{q_2}x}\zeta(0) \tag{E.5}$$

for ensuring that (E.3) holds on $t\in[0,\frac{1}{q_2}]$, and $w(1,t)$ to be

$$w(1,t)=e^{-\frac{d_4}{q_2}}\frac{c}{p}e^{\left(a+b\frac{c}{p}\right)\frac{1}{q_2}}e^{\left(a+b\frac{c}{p}\right)t}\zeta(0),\quad t\in[0,\infty) \tag{E.6}$$

for ensuring that (E.3) holds on $t\in[\frac{1}{q_2},\infty)$. If $c=0$, we obtain from (E.2), (E.5), (E.6) that $w[t]\equiv 0$ for $t\in[0,\infty)$. Together with $z[t]\equiv 0$ for $t\in[0,\infty)$, recalling (17), (E.4), $\zeta(0)\neq 0$ with (E.1), and $\lambda(1)\neq 0$ (according to (15), (A.11) with $c=0$, and (A.12)), it follows that $w(1,t)$ is not identically zero on $t\in[0,\infty)$: contradicts (E.6) under $c=0$. Next, we discuss the cases with $c\neq 0$. According to (17) and (E.4), $w(1,t)$ is piecewise-constant, which contradicts (E.6) that is an exponential function ($a+b\frac{c}{p}\neq 0$ ensured by Assumption 1). Therefore, Case 2 only happens when $\zeta(0)=0$, i.e., $z[t],w[t],\zeta(t)$ are identically zero on $t\in[0,\infty)$. It implies that $\Omega(t)$ is identically zero on $t\in[0,\infty)$, and $m(t)$ is exponentially convergent to zero recalling (6), (7), (19), (44), (46).

Case 3: We suppose that the estimate $\hat a(t)$ does not reach a in finite time. It implies that $\zeta[t]\equiv 0$ on $t\in[0,\infty)$ according to Claim 6. It means that $\beta(0,t)$ is identically zero on $t\in[0,\infty)$ according to (10), and then $\alpha(0,t)$ is identically zero on $t\in[0,\infty)$ according to (11). It follows that $\beta[t]$ is identically zero on $t\in[0,\infty)$, and $\alpha[t]$ is identically zero on $t\in[\frac{1}{q_1},\infty)$, recalling (12), (13). Therefore, for $t\in[\frac{1}{q_1},\infty)$, $\beta[t]$, $\alpha[t]$, $\zeta(t)$ are identically zero, i.e., $w[t]$, $z[t]$, $\zeta(t)$ are identically zero on $t\in[\frac{1}{q_1},\infty)$ recalling the inverse transformation (8), (9). Therefore, $\Omega(t)$ is identically zero on $t\in[\frac{1}{q_1},\infty)$, and $m(t)$ is exponentially convergent to zero, recalling (6), (7), (19), (44), (46).

The proof of Claim 7 is complete.

Authorized licensed use limited to: Xiamen University. Downloaded on March 16,2024 at 08:56:11 UTC from IEEE Xplore. Restrictions apply.

F. Proof of Claim 8.

We estimate the maximum value of t_ε in various situations of initial conditions $z[0], w[0], \zeta(0)$

Case 1: $z[0] \neq 0, w[0] = 0, \zeta(0) = 0$. According to (3), we have that $z[t], w[t]$ is not identically zero on $t \in [0, t_1]$ (if $w[t]$ is identically zero on $t \in [0, t_1]$, by virtue of (3) and $d_3 \neq 0$, it implies that $z[t]$ is identically zero on $t \in [0, t_1]$: contradiction). Suppose that $\zeta(t)$ is identically zero on $t \in [0, t_f]$, where $t_f = \min\{t_f : f \in \mathbb{Z}^+, t_f > \frac{1}{q_1} + \frac{1}{q_2}\}$. It means that $\beta(0,t)$ is identically zero on $t \in [0, t_f]$ according to (10), and then $\alpha(0,t)$ is identically zero on $t \in [0, t_f]$ according to (11). It follows that $\beta[t]$ is identically zero on $t \in [0, t_f - \frac{1}{q_2}]$, and $\alpha[t]$ is identically zero on $t \in [\frac{1}{q_1}, t_f]$, recalling (12), (13). Therefore, for $t \in [\frac{1}{q_1}, t_f - \frac{1}{q_2}]$, $\beta[t]$, $\alpha[t]$, $\zeta(t)$ are identically zero, i.e., $w[t]$, $z[t]$, $\zeta(t)$ are identically zero, recalling the inverse transformation (8), (9). According to (5), we have that U_d in (17) is kept constant in a time interval. Therefore, U_d is identically zero on $t \in [\frac{1}{q_1}, t_f - \frac{1}{q_2}]$, which implies that U_d is identically zero on $t \in [\frac{1}{q_1}, t_f]$. It follows that $z(x,t), w(x,t), \zeta(t)$ are identically zero for $t \in [\frac{1}{q_1}, t_f]$. By virtue of (1)–(5), (17), through iterative constructions between successive triggering times, we have that $U_d \equiv 0$ and $z(x,t), w(x,t), \zeta(t)$ are identically zero for $t \in [\frac{1}{q_1}, \infty)$. This implies that $\zeta(t) \equiv 0$ on $t \in [0, \infty)$ and that $\hat{a}$ does not reach the true value in finite time: contradiction. Therefore, the nonzero values of $\zeta(t)$ appear not later than t_f. Recalling Lemma 5, we have $\hat{d}_3(t_1) = d_3, \hat{d}_2(t_1) = d_2, \hat{a}(t_f) = a$. Therefore, $t_\varepsilon \leq T + \frac{1}{q_1} + \frac{1}{q_2}$, where T is the maximum dwell time between two triggering times.

Case 2: $w[0] \neq 0, z[0] = 0, \zeta(0) = 0$. The maximum time taken by the nonzero values of $w[0]$ propagate to z and $\zeta(t)$ is $\frac{1}{q_2}$. Therefore, the estimate $\hat{d}_3(t)$, $\hat{a}(t)$ would reach the true value d_3, a not later than $t_f = \min\{t_f : f \in \mathbb{Z}^+, t_f > \frac{1}{q_2}\}$ according to Lemmas 5, 6. Because of $w[0] \neq 0$, we have $\hat{d}_2(t_1) = d_2$. It follows that $t_\varepsilon \leq \frac{1}{q_2} + T$.

Case 3: $\zeta(0) \neq 0, z[0] = 0, w[0] = 0$. If $w[t]$ is identically zero on $t \in [0, t_1]$, this implies that $z[t]$ is identically zero on $t \in [0, t_1]$ according to (3) with $d_3 \neq 0$, which means that $\zeta(t)$ is identically zero on $t \in [0, t_1]$ by (4): contradiction. Therefore, $w[t]$ is not identically zero on $t \in [0, t_1]$. According to the proof in Case 2 of Claim 7, we know that the necessary condition of that $z[t]$ is identically zero on $t \in [0, t_f]$, where $t_f = \min\{t_f : f \in \mathbb{Z}^+, t_f > \frac{1}{q_2}\}$, is that w satisfies (E.5), (E.6), which implies $w[0] \neq 0$ $(c \neq 0)$ or $w[t] = 0$ for $t \in [0, t_1]$ $(c = 0)$: contradiction. Therefore, $z[t]$ is not identically zero on $t \in [0, t_f]$. Therefore, $\hat{d}_2(t_1) = d_2, \hat{a}(t_1) = a, \hat{d}_3(t_f) = d_3$. It follows that $\tau_\varepsilon \leq \frac{1}{q_2} + T$.

Case 4: $\zeta(0) \neq 0, w[0] \neq 0, z[0] = 0$. Suppose that $z[t]$ is identically zero on $t \in [0, t_f]$, where $t_f = \min\{t_f : f \in \mathbb{Z}^+, t_f > \frac{1}{q_2}\}$. According to the proof in Case 2 of Claim 7, if $c = 0$, a necessary condition of the above hypothesis is (E.5), which means $w[0] = 0$: contradiction. If $c \neq 0$, a necessary condition of the above hypothesis is (E.6) that does not hold, because the control input U_d applied at (E.4) is piecewise-constant while $w(1,t)$ in (E.6) is an exponential function ($a + b\frac{c}{p} \neq 0$ ensured by Assumption 1). Therefore, $z[t]$ is not identically zero on $t \in [0, t_f]$. This implies that $\hat{d}_3(\tau_f) = d_3$ according to Lemmas 5, 6. Because of $w[0] \neq 0$ and $\zeta(0) \neq 0$, we have $\hat{d}_2(t_1) = d_2$, $\hat{a}(t_1) = a$. Therefore, $t_\varepsilon \leq \frac{1}{q_2} + T$.

Case 5: $\zeta(0) \neq 0, z[0] \neq 0, w[0] = 0$. According to (3) with $d_3 \neq 0$, and the fact that $z[t]$ is not identically zero on $t \in [0, t_1]$, we have that $w[t]$ is not identically zero on $t \in [0, t_1]$. Recalling Lemma 5, we have $\hat{\theta}(t_1) = \theta$. Therefore, $t_\varepsilon \leq T$.

Case 6: $\zeta(0) = 0, z[0] \neq 0, w[0] \neq 0$. Following the analysis in Case 1, we have that the nonzero values of $\zeta(t)$ appears not later than t_f, where $t_f = \min\{t_f : f \in \mathbb{Z}^+, t_f > \frac{1}{q_1} + \frac{1}{q_2}\}$. Recalling Lemmas 5, 6, we have $\hat{d}_3(t_1) = d_3$, $\hat{d}_2(t_1) = d_2$, $\hat{a}(t_f) = a$. Therefore, $t_\varepsilon \leq T + \frac{1}{q_1} + \frac{1}{q_2}$.

Case 7: $\zeta(0) \neq 0, z[0] \neq 0, w[0] \neq 0$. According to Lemma 5, we have $t_\varepsilon \leq t_1 \leq T$.

Case 8: $z[0] = 0, w[0] = 0, \zeta(0) = 0$. According to the plant (1)–(5) with the control input (17), we know that $z[t], w[t], \zeta(t)$ are identically zero for $t \in [0, \infty)$. The estimates reach the true values in finite time only when $\hat{q}_1(0) = q_1, \hat{q}_2(0) = q_2$, i.e., $\tau_\varepsilon = 0$.

In summary, we have proved for all eight cases that $t_\varepsilon \leq \frac{1}{q_1} + \frac{1}{q_2} + T$. This completes the proof of Claim 8.

Acknowledgment

The authors would like to thank I. Karafyllis at National Technical University of Athens for his valuable comments on the portion of regulation-triggered batch least-squares identifier.

References

[1] H. Anfinsen and O. M. Aamo, *Adaptive Control of Hyperbolic PDEs*. Berlin, Germany: Springer, 2019.

[2] H. Anfinsen, H. Holta, and O. M. Aamo, "Adaptive control of a scalar 1-D linear hyperbolic PDE with uncertain transport speed using boundary sensing," in *Proc. Amer. Control Conf.*, 2020, pp. 1575–1581.

[3] H. Anfinsen, H. Holta, and O. M. Aamo, "Adaptive control of a linear hyperbolic PDE with uncertain transport speed and a spatially varying coefficient," in *Proc. 28th Mediterranean Conf. Control Autom.*, 2020, pp. 945–951.

[4] M. Bagheri, I. Karafyllis, P. Naseradinmousavi, and M. Krstic, "Adaptive control of a two-link robot using batch least-squares identifier," *IEEE/CCA J. Automatica Sinica*, vol. 8, no. 1, pp. 86–93, Jan. 2021.

[5] N. Bekiaris-Liberis, M. Jankovic, and M. Krstic, "Adaptive stabilization of LTI systems with distributed input delay," *Int. J. Adapt. Control Signal Process*, vol. 27, pp. 46–65, 2013.

[6] P. Bernard and M. Krstic, "Adaptive output-feedback stabilization of non-local hyperbolic PDEs," *Automatica*, vol. 50, pp. 2692–2699, 2014.

[7] D. Bresch-Pietri and M. Krstic, "Output-feedback adaptive control of a wave PDE with boundary anti-damping," *Automatica*, vol. 50, no. 5, pp. 1407–1415, 2014.

[8] J. M. Coron, R. Vazquez, M. Krstic, and G. Bastin, " Local exponential H^2 stabilization of a 2×2 quasilinear hyperbolic system using backstepping," *SIAM J. Control Optim.*, vol. 51, no. 3, pp. 2005–2035, 2013.

[9] M. A. Davo, D. Bresch-Pietri, C. Prieur,, and F. Di Meglio, "Stability analysis of a 2×2 linear hyperbolic system with a sampled-data controller via backstepping method and looped-functionals," *IEEE Trans. Autom. Control*, vol. 64, no. 4, pp. 1718–1725, Apr. 2019.

[10] J. Deutscher, "Finite-time output regulation for linear 2×2 hyperbolic systems using backstepping," *Automatica*, vol. 75, pp. 54–62, 2017.

[11] F. Di Meglio, F. Bribiesca-Argomedo, L. Hu, and M. Krstic, "Stabilization of coupled linear heterodirectional hyperbolic PDE-ODE systems," *Automatica*, 87, pp. 281–289, 2018.

Authorized licensed use limited to: Xiamen University. Downloaded on March 16,2024 at 08:56:11 UTC from IEEE Xplore. Restrictions apply.

[12] N. Espitia, "Observer-based event-triggered boundary control of a linear 2×2 hyperbolic systems," *Syst. Control Lett.*, vol. 138, 2020, Art. no. 104668.

[13] N. Espitia, A. Girard, N. Marchand, and C. Prieur, "Event-based control of linear hyperbolic systems of conservation laws," *Automatica*, vol. 70, pp. 275–287, 2016.

[14] N. Espitia, A. Girard, N. Marchand, and C. Prieur, "Event-based boundary control of a linear 2×2 hyperbolic system via backstepping approach," *IEEE Trans. Autom. Control*, vol. 63, no. 8, pp. 2686–2693, Aug. 2018.

[15] N. Espitia, I. Karafyllis, and M. Krstic, "Event-triggered boundary control of constant-parameter reaction-diffusion PDEs: A small-gain approach," *Automatica*, vol. 128, 2021, Art. no. 109562.

[16] E. Fridman and A. Blighovsky, " Robust sampled-data control of a class of semilinear parabolic systems," *Automatica*, vol. 48, no. 5, pp. 826–836, 2012.

[17] A. Girard, "Dynamic triggering mechanisms for event-triggered control," *IEEE Trans. Autom. Control*, vol. 60, no. 7, pp. 1992–1997, Jul. 2015.

[18] W. P. M. H. Heemels and M. C. F. Donkers, "Model-based periodic event-triggered control for linear systems," *Automatica*, vol. 49, pp. 698–711, 2013.

[19] W. P. M. H. Heemels, K. H. Johansson, and P. Tabuada, "An introduction to event-triggered and self-triggered control," in *Proc. 51st IEEE Conf. Decis. Control*, Maui, Hawaii, 2012, pp. 3270–3285.

[20] L. Hu, F. Di Meglio, R. Vazquez, and M. Krstic, "Control of homodirectional and general heterodirectional linear coupled hyperbolic PDEs," *IEEE Trans. Autom. Control*, vol. 61, no. 11, pp. 3301–3314, Nov. 2016.

[21] I. Karafyllis, M. Kontorinaki, and M. Krstic, "Adaptive control by regulation-triggered batch least squares," *IEEE Trans. Autom. Control*, vol. 65, no. 7, pp. 2842–2855, Jul. 2020.

[22] I. Karafyllis and M. Krstic, "Adaptive certainty-equivalence control with regulation-triggered finite-time least-squares identification," *IEEE Trans. Autom. Control*, vol. 63, pp. 3261–3275, Oct. 2018.

[23] I. Karafyllis, M. Krstic, and K. Chrysafi, "Adaptive boundary control of constant-parameter reaction-diffusion PDEs using regulation-triggered finite-time identification," *Automatica*, vol. 103, pp. 166–179, 2019.

[24] M. Krstic, *Delay Compensation for Nonlinear, Adaptive, and PDE Systems*. Berlin, Germany: Springer, 2009.

[25] M. Krstic, I. Kanellakopoulos, and P. Kokotovic, *Nonlinear and Adaptive Control Design*. Hoboken, NJ, USA: Wiley, 1995.

[26] M. Krstic and A. Smyshlyaev, "Adaptive boundary control for unstable parabolic PDEs—Part I: Lyapunov design," *IEEE Trans. Autom. Control*, vol. 53, no. 7, pp. 1575–1591, Aug. 2008.

[27] C. Prieur, A. Girard, and E. Witrant, "Stability of switched linear hyperbolic systems by Lyapunov techniques," *IEEE Trans. Autom. Control*, vol. 59, no. 8, pp. 2196–2202, Aug. 2014.

[28] C. Roman, D. Bresch-Pietri, C. Prieur, and O. Sename, "Robustness to in-domain viscous damping of a collocated boundary adaptive feedback law for an antidamped boundary wave PDE," *IEEE Trans. Autom. Control*, vol. 64, no. 8, pp. 3284–3299, Aug. 2019.

[29] A. Selivanov and E. Fridman, "Distributed event-triggered control of diffusion semilinear PDEs," *Automatica*, vol. 68, pp. 344–351, 2016.

[30] A. Seuret, C. Prieur, and N. Marchand, "Stability of non-linear systems by means of event-triggered sampling algorithms," *IMA J. Math. Control Inf.*, vol. 31, no. 3, pp. 415–433, 2014.

[31] A. Sezgin and M. Krstic, "Boundary backstepping control of flow-induced vibrations of a membrane at high mach numbers," *ASME J. Dyn. Syst., Meas. Control*, vol. 137, 2015, Art. no. 081003.

[32] A. Smyshlyaev and M. Krstic, "Adaptive boundary control for unstable parabolic PDEs-Part II: Estimation-based designs," *Automatica*, vol. 43, pp. 1543–1556, 2007.

[33] A. Smyshlyaev and M. Krstic, "Adaptive boundary control for unstable parabolic PDEs—Part III: Output feedback examples with swapping identifiers," *Automatica*, vol. 43, pp. 1557–1564, 2007.

[34] P. Tabuada, "Event-triggered real-time scheduling of stabilizing control tasks," *IEEE Trans. Autom. Control*, vol. 52, no. 9, pp. 1680–1685, Sep. 2007.

[35] A. Tanwani, C. Prieur, and M. Fiacchini, "Observer-based feedback stabilization of linear systems with event-triggered sampling and dynamic quantization," *Syst. Control Lett.*, vol. 94, pp. 46–56, 2016.

[36] R. Vazquez, M. Krstic, and J. M. Coron, "Backstepping boundary stabilization and state estimation of a 2×2 linear hyperbolic system," in *Proc. 50th IEEE Conf. Decis. Control Eur. Control Conf.*, 2011, pp. 4937–4942.

[37] J. Wang, S. Koga, Y. Pi, and M. Krstic, "Axial vibration suppression in a PDE model of ascending mining cable elevator," *ASME J. Dyn. Syst., Meas. Control*, vol. 140, 2018, Art. no. 111003.

[38] J. Wang and M. Krstic, "Vibration suppression for coupled wave PDEs in deep-sea construction," *IEEE Trans. Control Syst. Technol*., vol. 29, no. 4, pp. 1733–1749, Jul. 2021.

[39] J. Wang and M. Krstic, "Event-triggered output-feedback backstepping control of sandwich hyperbolic PDE systems," *IEEE Trans. Autom. Control*, vol. 67, no. 1, pp. 220–235, Jan. 2022.

[40] J. Wang and M. Krstic, "Regulation-triggered adaptive control of a hyperbolic PDE-ODE model with boundary interconnections," *Int. J. Adapt. Control Signal Process*, vol. 35, no. 8, pp. 1513–1543, 2021.

[41] J. Wang and M. Krstic, "Adaptive event-triggered PDE control for load-moving cable systems," *Automatica*, vol. 129, 2021, Art. no. 109637.

[42] J. Wang, M. Krstic, and I. Karafyllis, "Adaptive regulation-triggered control of hyperbolic PDEs by batch leastsquares," in *Proc. Amer. Control Conf.*, 2021, pp. 4057–4062.

[43] J. Wang, Y. Pi, and M. Krstic, "Balancing and suppression of oscillations of tension and cage in dual-cable mining elevators," *Automatica*, vol. 98, pp. 223–238, 2018.

[44] Z. Yao and N. H. El-Farra, "Resource-aware model predictive control of spatially distributed processes using event-triggered communication," in *Proc. 52nd IEEE Conf. Decis. Control*, 2013, pp. 3726–3731.

[45] H. Yu, R. Vazquez, and M. Krstic, "Adaptive output feedback control of flow-induced vibrations of a membrane at high mach numbers," in *Proc. 56th IEEE Conf. Decis. Control*, 2017, pp. 670–675.

Ji Wang (Member, IEEE) received the Ph.D. degree in mechanical engineering from Chongqing University, Chongqing, China, in 2018.

From 2019 to 2021, He was a Postdoctoral Scholar with the Department of Mechanical and Aerospace Engineering, University of California, San Diego, La Jolla, CA, USA. He is currently an Associate Professor with the Department of Automation, Xiamen University, Xiamen, China. His research interests include modeling and control of distributed parameter systems, with applications in string-actuated mechanisms.

Dr. Wang has been an Associate Editor for *Systems and Control Letters*, since 2021.

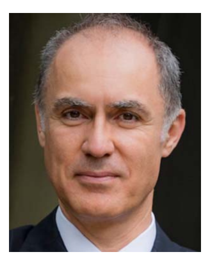

Miroslav Krstic (Fellow, IEEE) received the degree (summa cum laude) in electrical engineering from the Department of Electrical Engineering, University of Belgrade, Yugoslavia, in 1989, and the M.S. and Ph.D. degrees from the Department of Electrical and Computer Engineering, University of California, Santa Barbara, CA, USA, in 1992, and 1994, respectively.

He is currently Distinguished Professor of Mechanical and Aerospace Engineering, holds the Alspach endowed chair, and is the founding director of the Cymer Center for Control Systems and Dynamics at UC San Diego. He also serves as Senior Associate Vice Chancellor for Research at UCSD. He has coauthored 16 books on adaptive, nonlinear, and stochastic control, extremum seeking, control of PDE systems including turbulent flows, and control of delay systems.

Prof. Krstic has been elected Fellow of IEEE, IFAC, ASME, SIAM, AAAS, IET (UK), and AIAA (Assoc. Fellow) - and as a foreign member of the Serbian Academy of Sciences and Arts and of the Academy of Engineering of Serbia. He has received the Bellman Control Heritage Award, SIAM Reid Prize, ASME Oldenburger Medal, Nyquist Lecture Prize, Paynter Outstanding Investigator Award, Ragazzini Education Award, IFAC Nonlinear Control Systems Award, Chestnut textbook prize, Control Systems Society Distinguished Member Award, the PECASE, NSF Career, and ONR Young Investigator awards, the Schuck ('96 and '19) and Axelby paper prizes, and the first UCSD Research Award given to an engineer. He serves as Editor-in-Chief of Systems and Control Letters and has been serving as Senior Editor in *Automatica* and IEEE TRANSACTIONS ON AUTOMATIC CONTROL, as editor of two Springer book series, and has served as Vice President for Technical Activities of the IEEE Control Systems Society and as chair of the IEEE CSS Fellow Committee.

Authorized licensed use limited to: Xiamen University. Downloaded on March 16,2024 at 08:56:11 UTC from IEEE Xplore. Restrictions apply.